Review Article

The Application of Different Technologies for Removal of Rifampicin from Aquatic Environments: A Recent Review

Hatice ERDEM[*]

Muş Alparslan University, Department of Food Engineering, h.erdem@alparslan.edu.tr, Orcid No: 0000-0002-7666-8301

ARTICLE INFO	ABSTRACT
	Antibiotics are a group of drugs widely used as human and veterinary drugs and in aquaculture and agriculture. Recently, parent compounds and their metabolites are constantly excreted and released into environmental matrices, due to the fact that antibiotics cannot be completely metabolized after consumption by humans and animals and cannot be completely removed by conventional wastewater treatment plants. The accumulation and persistence of antibiotics in environmental matrices can lead to harmful effects on ecosystems, even at concentration levels as low as ng/L to µg/L. Rifampicin (RIF), which belongs to the macrocyclic antibiotic class, is the most important antibiotic widely used in the tuberculosis treatment. Lately, the RIF was detected in aquatic environments and needs to be removal effectively. This review considers the current state of knowledge regarding the sources, fate, effects and removal processes of the antibiotic RIF. In this review, the different treatment techniques such as adsorption, advanced oxidation processes (AOPs) and other technologies (membrane process and moving bed biofilm reactor) for RIF removal were evaluated and compared. A comparison between these techniques was made focusing on performance and efficiency. As a result, it was found that adsorption and AOPs were the most studied method and almost all of the studied RIF removal methods were also to be successful.

Introduction

The emerging pollutants are new chemicals or products that do not have regulatory policy and whose effects on the environment and human health are unknown, and have now become a serious environmental problem due to changing lifestyle patterns. These emerging pollutants usually involve personal care products, pesticides, endocrine disruptors, microplastics and pharmaceuticals [1, 2]. Pharmaceuticals among emerging pollutants have been a turning point in the development of human scientific, and have prolonged life span, saved millions of people from fatal diseases and improved the quality of life. This success has resulted in their emergence as rapidly growing environmental pollutants. In the last three decades, residues of pharmaceuticals have been detected in almost all environmental matrices on every continent, including the polar regions which have the world's most pristine environment. These environmental matrices include surface waters, groundwaters, wastewater treatment plant influents and effluents, and sludge. Pharmaceutical pollutants widely are visible in the geosphere and biosphere, and their concentrations are in a wide range. Variable degradation rates result in limited degradation both in the natural environment and in wastewater treatment plants. Although most pharmaceuticals are not enormously persistent, their constant release into the environment in small but important amounts from different sources makes a lots of them "pseudo-persistent" [3].

Pharmaceutical compounds can be classified into different classes such as antibiotics, anti-inflammatory, antidepressants, hormones, beta-blockers, antiepileptic, contrast products, statins, etc. [2]. The term "antibiotic" is used to refer to any class of organic molecules that inhibits or kills microbes through specific interactions with bacterial targets, regardless of the origin of a particular compound or class [4]. Antibiotics can be grouped according to their chemical structure or mechanism of action. These are a diverse group of chemicals that can be divided into different subgroups such as macrolides, β-lactams, sulfonamides, tetracyclines, quinolones, and others [5]. Antibiotics are continuously excreted and discharged into the environment from anthropogenic sources such as wastewater treatment plants due to their overuse and misuse for human (domestic and hospital use), veterinary and agricultural purposes. The introduction of these compounds into the environment through anthropogenic sources can pose a potential risk to aquatic and terrestrial organisms. The presence of antibiotics in the environment, even at their low concentration levels (ng/L - µg/L), was associated with a

prevalence of chronic toxicity and resistance to antibiotics in bacterial populations, making them ineffective in the treatment of several diseases in the near future [4, 6].

Rifampicin (RIF) is one of the most potent broad-spectrum antibiotics against bacterial pathogens and is used as a first-line drug to treat tuberculosis, as well as against diseases such as HIV, cancer, leprosy, and Alzheimer [7, 8]. In addition, a recent study revealed that RIF has good binding affinity with the COVID-19 protease and therefore can be used as prophylaxis and therapeutic treatment for corona patients [9]. After RIF enters the body, it is partly digested and the excessive amount is excreted in the faeces or urine. Lately, RIF was detected in wastewater from sewage treatment plants. However, RIF antibiotic contaminant cannot be completely removed in existing treatment systems due to its stability in the environment, high solubility in aqueous media and low bioavailability. RIF leakage into surface water, groundwater and sediments during production or application stages can possibly cause endocrine disorders and chronic toxicity in aquatic organisms and humans. It has also been found that RIF residues in the aquatic ecosystem can lead to the formation of antibiotic resistant genes (ARGs) in fish pathogens, the development of resistance to antibiotics, the alteration of microbial communities, and the potential transmission of ARGs to pathogens of humans as well as terrestrial animals [10]. Therefore, it is necessary to choose an efficient, easy-to-operate, cost-effective and environmentally friendly approach to the removal of RIF. According to the author' knowledge, any review article on the methods for the removal of antibiotic RIF have not yet been published. Therefore, the purpose of this review paper is to compare the different treatment processes used in the literature to date for the removal of RIF from aqueous matrices and thus provide insights for researchers in their future studies.
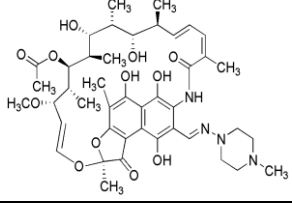
Rifampicin and its impacts on the environment and humans

RIF, 3-[(4-methyl-1-piperazinyl)imino]methyl rifamycin, also known as rifampin, belongs to the class of macrocyclic antibiotics containing a naphthohydroquinone ring spanned by a highly substituted aliphatic bridge, and the type and location of the substituent on their aromatic ring are different from each other. RIF is the most important antibiotic widely used in the treatment of tuberculosis, Hansen's disease, and other serious infections such as HIV, which inhibits bacterial DNA-dependent RNA polymerase [11].

RIF, the first antibiotic of the ansamycin family, was isolated in 1959 and entered into therapy in 1962 [12]. RIF was approved by the Food and Drug Administration (FDA) in 1971 for the treatment of patients with tuberculosis and asymptomatic carriers of Neisseria meningitides, and these are still the only approved indications [13]. RIF is also used by the government health program as an adjuvant in the treatment of immunocompromised patients and is on the World Health Organization (WHO) Essential Medicines List, the most important medications needed in the basic health system [14-16]. RIF is a limit Class II drug,

according to the Biopharmaceutical Classification System (BCS). RIF exhibits amphiphilic properties due to its chemical structure with very low pH-dependent aqueous solubility and poor stability in aqueous media [17]. RIF has zwitterionic nature with a pKa_1 of 1.7 related to the 4-hydroxyl group and a pKa_2 of 7.9 related to the 3-piperazine nitrogen, with an isoelectric point at pH 4.8 in aqueous solution [18]. Molecular structure and physicochemical properties of RIF are given in Table 1. RIF is relatively non-toxic [18]. However, a high dose of RIF can be toxic to biological systems and cause various side effects such as allergic reactions, nausea, diarrhea, vomiting, hepatotoxicity, loss of appetite, immunological disturbances, oxidative conjunctivitis, fatigue, headache and organic brain syndrome [19, 20].

Table 1. Physicochemical properties and molecular structure of RIF

CAS No.	13292-46-1
Molecular structure	
Molecular formula	$C_{43}H_{58}N_4O_{12}$
Molecular weight (g/mol)	822.953
Log Kow	4.24
pKa	1.70, 7.90
Solubility (H_2O, mg/mL)	1.4

Once in the body, RIF is partly digested and the its excess is excreted by humans through urine and faeces to the sewage systems, and was detected in effluents from wastewater treatment plants since the conventional treatment plants cannot effectively remove this type of resistant compounds [21]. It is of great concern that if RIF leaches into surface and groundwater, it can be a cause of chronic toxicity for humans and aquatic species [22]. RIF was detected at concentrations of 112.37–211 ng/g in sediments of the Dagu River [23], and at an average concentration of 0.3 ng/L with a 20% detection frequency in aquaculture ponds located in Dongying City, Shandong Province, in China [24]. RIF applied in shrimp rearing in coastal wetland of Cangio District (Hochiminhi City, Vietnam) was detected both in rearing ponds and outlet as 0.19–0.23 and 0.24–16.5 µg/l, respectively [25].

RIF can be used for the control of bacterial diseases (e.g., columnaris disease) in fish caused by bacterial and viral infection. Because RIF is a fat-soluble compound, RIF can enter into the body easily. It produces residues in the edible tissues of fish products and hereby can be harmful for human health. It can also lead to drug resistance in the

human body [19]. Studies on RIF residues in the aquaculture environment have shown that RIF with a high risk of developing resistance leads to ARGs in fish pathogens, increases antibiotic resistance, alters the microbial community, and potentially transfers ARGs to terrestrial animal and human pathogens [26, 27]. Huang et al. [28] detected 310 - 6.1×10^4 CFU/mL of rifampicin-resistant bacteria with average percentages of 11% in the effluent of a wastewater treatment plant in China. In addition, hepatoxicity caused by anti-tuberculosis drugs was documented in many studies [29, 30]. The effect of RIF on the metabonomic profile of rat urine and its relation to the traditional toxicity assessment of blood biochemical markers and histopathology was investigated and RIF was found to cause hapatoxicity [31]. A 2-month regimen of RIF and pyrazinamide for the treatment of tuberculosis was found to be effective, but causes hepatotoxicity of increasing severity [32].

Different technologies for removal of rifampicin

Adsorption

Adsorption is the mechanism in which an ion or molecule in the liquid or gaseous bulk phase stays on the surface of a solid. Here the ion or molecule is an adsorbate and the solid using for adsorption is called as an adsorbent. A liquid is rarely used as an adsorbent. Adsorption is a surface phenomenon involving only the adsorbent surface, and the adsorbate should not penetrate inside the adsorbent structure. The reverse mechanism, i.e. the separation of a molecule from the adsorbent surface, is called as desorption [33]. Adsorption was one of the most efficient, promising and widely used processes for the removal of pharmaceutical pollutants from waters due to its low initial investment, operational simplicity, non-selective nature and also not causing the formation of hazardous products [34]. Diverse porous materials such as activated carbon, zeolite, silica, resin, clay, graphene oxide, multi-walled carbon nanotubes and chitosan were investigated to improve the adsorption capacity of pharmaceuticals on adsorbents. The main adsorbents used to remove pharmaceuticals from wastewater are given in Figure 1 [35]. In this section, a review of adsorption studies in the literature for RIF removal is discussed and important outlines of these studies reported in recent years are presented.
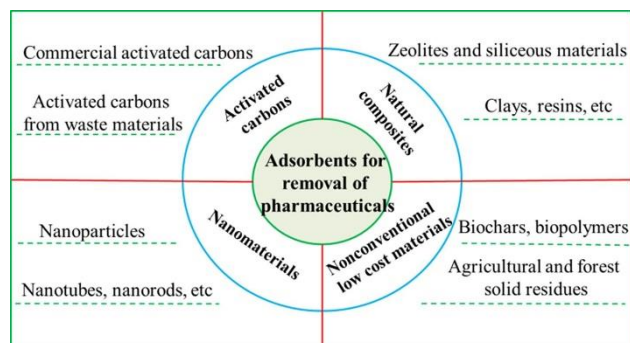

Figure 1. Main adsorbents used to remove pharmaceuticals from wastewater [35].

Among the adsorbents, activated carbons (ACs) have received more attention by reason of their better adsorption performances than other adsorbents. ACs are defined as a carbonaceous solid with high surface area, high micropore volume, and high adsorption capacity. Due to these characteristics, ACs are classified as an effective adsorbent for air pollution control and water treatment. Appropriate application of AC is dependent on its properties that vary with the type of raw precursor used and the technique of preparation. Commonly used materials for synthesis of ACs are natural coal, petroleum residue and wood due to their high carbon content. Recently, the production of activated carbon from agro-industrial wastes for a less costly adsorption system was on the focus of researchers [36]. In a study, the AC was prepared and characterized by $ZnCl_2$ activation using vine shoots (*vitis vinifera*) which is a lignocellulosic and low cost precursor. Then, adsorption experiments were carried out by selecting RIF as the target pollutant to determine the adsorption capacity of the prepared AC. It was reported that the pore size, surface area and pore volume of AC increased with increasing impregnation rate and temperature, reaching a maximum at an impregnation rate of 40/30 (precursor/$ZnCl_2$) at 700 °C. Under optimum conditions, it was found that the activated carbon has the total pore volume of 0.842 cm^3/g, BET surface area of 1689 m^2/g, iodine number of 1276 mg/g and the point of zero charge (pH_{PZC}) of 4.8 as well as high carbon content (89.65%), acidic functional groups (total 0.2516 meq/g) and a very porous surface. It was observed that the RIF removal yield increased with the increase of AC dosage and contact time, while it decreased with increasing initial dosage of RIF. It was determined that the adsorption data best matched the Langmuir adsorption isotherm and the maximum adsorption capacity was found to be 476.2 mg/g. As a result, it was reported that the quality AC can be produced with $ZnCl_2$ activation from vine shoots [37].

In another study, the activated carbon cocoa shells (ACCS) were applied as a biosorbent to remove RIF antibiotics from industrial effluents. It was observed that the ACCS surface had an irregular and coarse structure before RIF adsorption, and the structure of the cocoa shells did not change significantly after RIF adsorption. The contact time to reach the equilibrium between adsorbent and adsorbate was found to be a minimum of 2 hours. It was determined that the effect of temperature on adsorption was low. Whereas the percentage of RIF removal efficiency increased with the increase of adsorbent dosage, but decreased in excessive adsorbent dosage (> 0.3 g/L). It was explained as the reason for this that higher dosage leads to aggregation of particles and repulsive forces between the binding sites, resulting in reduced interaction of RIF with the adsorbent and a decrease in the total surface area of the adsorbent. When the effect of pH on RIF removal efficiency was investigated in the pH range of 5-10.5, it was determined that the yield decreased with increasing pH (> 6). It was stated that this effect can be due to the surface charge of adsorbent (pH_{PZC}: 6.8) and that RIF molecules were converted from protonated, zwiteronic to anionic form during the transition from acidic to neutral and alkaline solutions. It was

concluded that the mechanisms controlling the adsorption of RIF on ACCS can be attributed to a combination of bond formation, hydrogen bonds, electrostatic interaction and hydrophobic interaction. It was found that the Freundlich isotherm model and the general order kinetic model ensured the best fit to the experimental data, and negative enthalpy indicated an exothermic process occurring through physisorption. From the obtained experimental data, it was concluded that the isosteric heat values decreased with the increase of the surface coating, indicating the existence of strong interactions between RIF and cocoa shell [38].

Mytella falcata shells (a bivalve mollusk), which has recently caught the attention of Brazilian researchers by cause of its high abundance and polluting potential, were used as a biosorbent for the antibiotic RIF removal from water. *Mytella falcata* shells were tested raw or after either pyrolysis or calcination (700 °C) to increase adsorption capacity. As a result of characterization studies, aragonite and calcite, which reflect the composition of *Mytella falcata* shells, were found to be mainly crystalline calcium carbonate ($CaCO_3$) forms of calcined *Mytella falcata* shells. The pH_{PZC} of the adsorbent was determined as 11.80. After pyrolysis and even more after calcination, irregular particles of reduced size were observed, after which a more regular size shape was obtained. It was stated that this was an indicative of the change of material structure as it goes through the heat treatment processes. It was determined that calcined *Mytella falcata* shells have a high concentration of calcium (Ca) and compounds such as Sr, Si and K in much smaller proportions. The affinity of the raw, pyrolyzed or calcined *Mytella falcata* shells for RIF was preliminary tested and the calcined *Mytella falcate* shells were found to show the highest removal efficiency (78 ± 0.2). RIF is a non-polar molecule (polarity: Log P 3.719), solution pH changes its solubility, but was observed to have little effect on its adsorption on calcined *Mytella falcata* shells. It was explained that this result is related to the pH_{PZC} of the adsorbent and the amphoteric properties of RIF. Therefore, it was stated that the substance can interact with the solid surface both below and above pH 11.8 (pH_{PZC}). In addition, the equilibrium data showed that the RIF adsorption capacity was independent of temperature, probably due to the increase in the simultaneous water desorption with the increase in temperature. Experimental data showed a better fit to the pseudo-first order kinetic model. The obtained data from isotherm results fitted better to the Redlich-Peterson model, which is characterized by the multilayer adsorption hypothesis with non-uniform heat distribution. Thermodynamic parameters showed that the adsorption process was spontaneous and slightly endothermic. Further adsorption tests were conducted to investigate the effect of ionic strength; it was concluded that an important increase of about 15% in the salt concentration in the medium promoted RIF adsorption on calcined *Mytella falcata* shells. Adsorbent regeneration tests by sonication showed a important decrease of process performance after 5 adsorption/desorption cycles [21].

Rusu et al. developed 6 types of eco-friendly biosorbents (SC-A-5%, SP-A-5%, SC-C-2.5%, SP-C-2.5%, SPRMB-A-5% and SPRMB-A-9%) by immobilizing *Saccharomyces cerevisiae*, *Saccharomyces pastorianus* and *Saccharomyces pastorianus* residual biomass on natural polymers (alginate and chitosan) and evaluated their biosorptive potential for removal of three drugs (cephalexin, rifampicin, ethacridine lactate) and two dyes (orange II and indigo carmine). It was determined that the synthesized biosorbents lost their sphericity but it was less accentuated for the materials obtained by the immobilization of *Saccharomyces cerevisiae* ve *Saccharomyces pastorianus* on alginate than those on chitosan, and this behavior was due to the removal of water during drying. While similar proportions of carbon, nitrogen and oxygen were present in all biosorbents, there were differences in the percentages of sodium and calcium according to the preparation methods. pH_{PZC} values for biosorbents prepared with sodium alginate were lower than the values for biosorbents prepared on chitosan bentonite (6.9 for SC-A-5%, 6.6 for SP-A-5%, 6.9 for SPRMBA-5% and 6.8 for SPRBM-A-9%, 8.3 for SC-C-2.5% and 8.8 for SP-C-2.5%). Collected data indicated that the best values for RIF removal was obtained for biosorbents containing chitosan as polymeric matrix (24.70 mg/g for SC-C-2.5% and 24.89 mg/g for SP-C-2.5%). It was reported that electrostatic and π-π interactions and hydrogen bonding between RIF and biosorbents can be responsible for biosorption. As a result, it was stated that the removal efficiency depended on the type of polymer used for immobilization [39].

Nanoscale iron particles (Fe NPs) with large surface areas and high surface reactivity are next-generation environmental remediation technologies that can provide cost-effective solutions. Equally important, Fe NPs provide tremendous flexibility for in-situ applications and researches have shown that they are very effective to remove a wide variety of common environmental pollutants [40]. Lin et al. aimed to simultaneously removal of RIF and Pb(II) by Fe NPs produced using a green tea extract. The synthesized Fe NPs were mainly amorphous, suggesting that organic molecules from the green tea extract successfully combined with Fe NPs and covered the surface of Fe NPs. When the surface composition and elemental distribution of Fe NPs were examined, it was found that the original Fe NPs consisted only of C, O, and Fe, and after the reaction, an important new Pb element (15.1%) formed, consistent with the Pb(II) adsorption by the Fe NPs. Before exposure to pollutants, the exterior of the Fe NPs was relatively rough, and the nanoparticles were uniformly dispersed and exist in the form of chains. In contrast, after exposure to pollutants, Fe NPs showed a large amount of agglomeration and the morphology became coarser, which was associated with RIF and Pb(II) adsorbing to the Fe NPs surface. The specific surface area of Fe NPs was calculated as 37.3 m^2/g (meso/macro porous). The adsorption of both Pb(II) and RIF by Fe NPs best fitted pseudo-second order kinetics in which the adsorption process was mainly by chemisorption. The probable mechanism of the simultaneous Pb(II) and RIF removal by Fe NPs was explained by the those two strategies: a) Pb(II) was adsorbed to the Fe NPs surface thanks to the natural

adsorption properties of iron oxides for metal ions, b) RIF and Pb(II) interacted more specifically with functional groups on the Fe NPs surface. As a result of experiments performed with real wastewater samples, it was determined that both pollutants were successfully removed (97.5% of Pb(II) and 68.8% of RIF) in a short time (20 min) by Fe NPs. Adsorbent reusability analysis suggested that even after 5 cycles, Fe NPs showed relatively high yields (52.3% of Pb(II) and 64.9% of RIF) and were highly reusable [41].

Green synthesized magnetic Fe_3O_4 nanoparticles by *Excoecaria cochinchinensis* extract were applied as a novel technology for RIF removal. The RIF adsorption efficiency of commercial Fe_3O_4 and green synthesized Fe_3O_4 were compared, and the removal efficiency of green synthesized Fe_3O_4 was found to be quite high, since the interaction between commercial Fe_3O_4 and RIF is mild and unstable, coupled with simultaneous adsorption and desorption processes. SEM images showed that different shapes and particle sizes were formed by spherical nanoparticles agglomerated in diameter range of 20-30 nm. The zeta potentials of Fe_3O_4 were determined in the solution pH range of 4-10, and Fe_3O_4 was found to be negatively charged at all solution pHs. The BET-specific surface area, a volume of pores and an average pore size of prepared Fe_3O_4 was found to be 111.8 m^2/g, 9.06 cm^3/g and 6-7 nm, respectively. It was determined that the adsorbent dosage, temperature and initial pH parameters significantly affected the RIF removal efficiency. The increase in the adsorption rate with the increase in temperature showed that the adsorption process was endothermic. It was found that RIF removal increased when pH increased from 4 to 5.5, whereas it decreased when pH increased from 5.5 to 10. This was attributed to the fact that the pH change can remarkably affect the surface charge of Fe_3O_4, and also RIF has two pKa. When the pH was higher than 5.5, the OH^- concentration in the reaction system continued to rise, the negative charge on the Fe_3O_4 surface increased. Therefore, the electrostatic adsorption was strongest at the 5.5 of pH and the RIF was zwitterion at this point. The interaction between RIF and Fe_3O_4 was predicted to inhibit or promote removal efficiency. The kinetic studies showed that the pseudo second-order model fitted for the adsorption process well and the Langmuir model was better to explain the adsorption of RIF by Fe_3O_4. The calculated activation energy value (E_a: 32.46 kJ/mol) showed that the adsorption process was mainly chemisorption. In the light of characterization and batch experiments, it was suggested that the adsorption mechanism of RIF on Fe_3O_4 nanoparticles can be electrostatic attraction and adsorption reaction between RIF and Fe_3O_4 active surface sites. Reusability tests of Fe_3O_4 for RIF adsorption showed that the removal efficiency dropped to 61.5% after five cycles. The application of Fe_3O_4 for the removal of RIF from real wastewater samples was investigated and within 1 h 82.5% and 76.0% of RIF was removed from municipal and aquaculture wastewaters, respectively [27].

Various materials (graphene, iron-based materials, metal/metal oxide nanoparticles and modified metal composites, etc.) used in the removal of antibiotics have some restrictions. For instance, graphene adsorbs the pollutant that can then become a secondary pollution source, metal/metal oxide NPs can release trace amounts of toxic heavy metals into the environment and iron-based materials tend to aggregate, all of which disrupts ecosystems. To overcome these limitations, the focus was on the production of non-agglomerated, non-toxic, modified iron-based materials for the removal of antibiotic contaminants such as RIF. Xu et al. prepared a hybrid RGO@Fe/Pd composite by one-step green synthesis using a green tea extract for RIF removal. The best conditions for the synthesis of RGO@Fe/Pd were determined as Fe/Pd: 100/5 and GO/Fe: 1/1. Characterization analyzes revealed that the elemental composition of RGO@Fe/Pd consisted of Pd (28.1%) and Fe (2.96%), and Fe on RGO@Fe/Pd was in an oxidized state while Pd was in the divalent (Pd^{2+}) and zerovalent (Pd^0) states. 96.1% RIF removal was achieved by RGO@Fe/Pd having a surface area of 48.14 m^2/g. It was determined that RGO@Fe/Pd removed RIF by adsorption and reduction, and catechol and caffeine were the two main biomolecules involved in the reduction process [42]. In another study using RGO@Fe/Pd, parameters affecting RIF removal, adsorption and reduction kinetics, and RIF degradation mechanism were investigated. RGO@Fe/Pd dosage, initial RIF concentrations, pH and temperature were found to affect the removal process. It was determined that the removal efficiency increased when the pH was increased from 5 to 7, whereas the removal efficiency decreased by approximately 20% at pH 9. This difference in removal efficiencies was attributed to the fact that RIF has two different pKa. It was estimated that the removal efficiency was higher at pH 7 due to the negatively charged hybrid material, but decreased when RIF was negatively charged at pH 9. It was reported that rGO@Fe/Pd remained stable at relatively high temperatures and did not lose its functionality. Optimal isothermal adsorption parameters for RIF by rGO@Fe/Pd NPs demostrated that the process comply with a Freundlich-type adsorption, pointing out that multilayer adsorption had occurred. However, it was suggested that since the pKa values of RIF are both between pH 1.7 and 7.9, RIF would have a double charge under experimental conditions and the adsorption process would use electrostatic attraction. The E_a value was calculated 33.15 kJ/mol, proving that the adsorption occured mainly by chemisorption. Adsorption and reduction kinetics showed that RIF followed a pseudo-second order model. A mechanism for RIF degradation based upon adsorption and catalytic reduction was proposed. It was determined that the RIF was reduced with nano iron, and nano palladium acted as a catalyst during this process. It was concluded that RIF degradation was incomplete and only converted to slightly smaller molecules, and therefore more studies are needed for complete degradation of RIF and to avoid exposure to intermediates of unknown toxicity. In addition, the practical removal yield of RIF in municipal sewage (58.1%) and aquaculture sewage water (71.9%) was successfully verified [43].

Xue et al. [44] prepared a hybrid bimetallic Fe/Ni nanoparticles and reduced graphene supported bimetallic Fe/Ni nanoparticles (Fe/Ni-rGO) and evaluated them for

simultaneous Pb and RIF removal. The removal efficiency of Fe/Ni-rGO was higher than rGO, nFe/Ni or Fe-rGO. Compared to the single pollutant systems (i.e. RIF or Pb(II) added in isolation), the removal of both RIF and Pb(II) in the mixed pollutant system were reduced. It was suggested that this was from competitive adsorption and reduction between RIF and Pb(II) in the mixed pollutant system. Exhaustive characterization and analysis of Fe/Ni-rGO showed that both Fe and Ni nanoparticles were evenly dispersed on the rGO surface, and the aggregation of Fe, Ni nanoparticles and stacking of rGO were reduced in the hybrid. LC-TOF-MS analysis demonstrated that RIF degraded to small-molecule fragments and the degradation process was incomplete. The adsorption of RIF was found to best fit a pseudo-second order kinetic model and the Freundlich isotherm model. It was proposed that the mechanism for simultaneous RIF and Pb(II) removal by Fe/Ni-rGO included surface adsorption on rGO followed by catalytic reduction of RIF by surface-coated Fe/Ni bimetallic nanoparticles. After 5 cycles, the removal of RIF by Fe/Ni-rGO decreased from 84.6% to 75.4%, confirming the good reusability of Fe/Ni-rGO.

Shafaati et al. synthesized chitosan/Fe_3O_4 grafted graphene oxide (CS/Fe_3O_4/GO) nanocomposite and used for RIF adsorption to evaluate its effectiveness. It was determined that the GO/CS/Fe_3O_4 composite consisted of oxygen (26.1%), carbon (6.8%), iron (65.9%) and nitrogen (1.8%). On this basis, the iron signal in the GO/CS/Fe_3O_4 composite was attributed to the presence of Fe_3O_4 and the nitrogen signal to the presence of CS. When the magnetic property of naked Fe_3O_4 and GO/CS/Fe_3O_4 composite was measured using a vibrating sample magnetometer at room temperature, the magnetic saturation (Ms) of GO/CS/Fe_3O_4 was 49.8 emu/g, which was lower than that of Fe_3O_4 (57.6 emu/g). This decrease was associated with the relatively smaller particle size of the Fe_3O_4 particles in naked Fe_3O_4 and the quenching of the magnetic moment by the interaction between the CS and GO coating layers and the surface of the Fe_3O_4 particles. BET surface area, average pore diameter, pore volume, and pH_{PZC} of GO/CS/Fe_3O_4 was calculated 96.14 m^2/g, 8.1248 nm, 0.1953 cm^3/g and 5, respectively. The effects of experimental parameters on adsorption efficiency were investigated by batch experiments. With an increase in solution pH from 3 to 5, both the the removal efficiency and adsorption capacity improved and reached the maximum, which can be explained by increase in the electrostatic interaction between the $RIF^{\pm}$ zwitterions and the positively charged surface of the adsorbent. On the other hand, it was reported that with a greater increase of pH from 6 to 9, the adsorption capacity and RIF removal was significantly reduced due to the electrostatic repulsion between RIF^- and the negatively charged adsorbent surface, which inhibited adsorption of RIF. However, it was suggested that adsorption of RIF can occur through hydrophobic interactions, and the π–π stacking interaction between the aromatic rings of RIF and the delocalized-π electron systems of GO on GO/CS/Fe_3O_4. The increase of removal efficiency with increased temperature was ascribed to the increase in the diffusion rate of RIF molecules to the inner GO/CS/Fe_3O_4 pores and

the boundary layer, and to the decrease in fluid viscosity facilitating the motion of RIF molecules towards the active adsorbent sites. It was determined that the increase in sodium chloride (NaCl) concentration, which was used to examinate the effect of ionic strength on RIF adsorption, decreased the efficiency of RIF removal. It was stated that this was due to the fact that Cl^- ions was probably in competition with RIF ions to occupy the available adsorption sites. RIF adsorption on GO/CS/Fe_3O_4 showed the highest fit with the second-order kinetic model and the Langmuir isotherm model. Thermodynamic studies have exhibited the endothermic and spontaneous nature of RIF adsorption. GO/CS/Fe_3O_4 showed satisfactory regeneration performance with high removal efficiency (> 70%) after seven cycles of adsorption-desorption. In addition, real water samples to research the practical use of GO/CS/Fe_3O_4 to adsorb RIF in contaminated waters were used as models in adsorption tests without pretreatment, and it was concluded that the groundwater matrix did not have a important effect on the adsorption process [10].

Abbasi et al. [45] investigated the uptake and release properties of RIF by ultrasound-assisted synthesized Cu-BTC nanoparticles, by comparing them with activated carbon and bulk Cu-BTC. It was determined that the amount of RIF adsorbed on nano Cu–BTC was much higher than that on bulk Cu–BTC and activated carbon. It was clearly verified that when XRPD models were investigated to confirm the crystal structure of the adsorbent, the Cu-MOF particles were successfully prepared by ultrasound irradiation. Silva et al. [46] synthesized MgFe Layer Double Hydroxides (LDH) by co-precipitation, ultrasound irradiation, hydrothermal and microwave methods. Considering the synthesis time, crystallinity, surface area, volume and diameter of the pores, and the percent removal of RIF, the ultrasound followed by hydrothermal (U-H) method was found to be the best material among the synthesis methods. In another study, green nanoemulsion (GNE) multiple components (N1-N5) were used to remove RIF from contaminated aqueous bulk solution. The highest removal efficiency value (91.7%) was obtained with NF5 in correlation with the lowest size (maximum surface area available for contact adsorption) value (~39 nm), polydispersity index (0.112) and viscosity (82 cP) [47].

As can be seen from the above-mentioned data, the different adsorbents used for the adsorption of RIF have been quite successful. The most studied adsorbents for RIF adsorption were nanoparticles, activated carbons, and hybrid materials consisting of carbonaceous and metal-based materials. The results of the researchers' studies demonstrated that the characteristics of the adsorbent (surface area, pore diameter, pore volume, pH_{PZC}, etc.), the physicochemical properties of RIF (e.g., pKa) and operating parameters of process (temperature, pH, etc.) affect the RIF removal. The main adsorption mechanisms were hydrogen bonding, electrostatic attraction/interaction and π–π interaction. However, no information was given on the disposal of the used adsorbents after application. Table 2 and Table 3 provides a comparison of different adsorbents reported for RIF removal in the literature.

Tablo 2. Comparison of different adsorbents reported for RIF removal in the literature.

Adsorbent	S_{BET} (m²/g)	Conditions	Removal (%)	Isotherms	Kinetics	Adsorption capacity (mg/g)	Ref.
GO/CS/Fe₃O₄ nanocomposite	96.14	RIF:20 mg/L, GO/CS/Fe₃O₄: 0.5 g/L, pH: 5, 55 °C, 75 min	95	Langmuir	Pseudo-second order model	102.11	[10]
Calcined *Mytella falcata* shells	-	RIF: 100 mg/L, biosorbent: 0.2 g, 30 °C, pH: 13, 30-45 min	96	Redlich-Peterson model	The pseudo-first order model	≅10	[21]
Nano-Fe₃O₄	111.8	RIF: 20 M, nanoFe₂O₃: 10 mg, pH: 5.5, 30 °C, 90 min	98.4	Langmuir	Pseudo-second order model	84.80	[27]
Activated Carbon from Vine Shoots	1689	RIF: 500 mg/L, AC: 5 g/L, pH: 7, 25 °C, 30 min	88	Langmuir	-	476.2	[37]
Activated carbon cocoa shells (ACCS)	-	RIF:10 mg/L, ACCS: 0.3 g/L, pH: 6, 20 °C, 120 min	80	Freundlich	Pseudo n-order model	26.66	[38]
Biosorbents (SC-C-2.5%) (SP-C-2.5%)	-	RIF: 50 mg/L, Biosorbents: 1g/25 mL, pH: 6, 12 h, ambient temperature	-	-	-	24.70 (SC-C-2.5%), 24.89 (SP-C-2.5%)	[39]
Fe-NPs	37.3	RIF:50 mg/L, Fe-NPs: 0.5 g/L, pH: 3-5, 20-40 °C, 120 min	91.6	Freundlich	Pseudo-second order model	107.70	[41]
rGO@Fe/Pd	48.14	RIF:20 mg/L, rGO@Fe/Pd: 0.2 g/L, pH: 7, 30 °C, 20 min	96.1	-	-	-	[42]
rGO@nFe/Pd	-	RIF: 20 mg/L, rGO@Fe/Pd: 0.2 g/L, pH: 7, 30 °C, 20 min	89	Freundlich	Pseudo-second order model	90.9	[43]
Fe/Ni-rGO	-	RIF: 50 mg/L, Fe/Ni-rGO: 1.6 g/L, pH: 5.1, 30 °C, 180 min	96.8	Freundlich	Pseudo-second order model	27.92	[44]
Cu-BTC MOF	376.4	RIF: 0.17 mmol, Cu–BTC: 13 mg/50 mL, 48 h	-	-	-	42.15	[45]
MgFe/LDH	82.1 (U-H) 75.1 (M-H)	RIF: 0.05 mg/L, MgFe/LDH: 5 g/L, 24 h	82.7 (U-H) 82.5 (M-H)	-	-	9.33 (U-H) 9.16 (M-H)	[46]

Table 3. Thermodynamic parameters for rifampicin adsorption reported for RIF removal in the literature.

Adsorbent	Temperature (°C)	ΔG° (kJ/mol)	ΔH° (kJ/mol)	ΔS° (kJ/mol)	Ref.
GO/CS/Fe₃O₄ nanocomposite	25	-13.41	18.63	0.107	[10]
	35	-14.48			
	45	-15.56			
	55	-16.63			
Calcined *Mytella falcata* shell	30	-29.28	1.65	-1.101	[21]
	40	-29.59			
	50	-31.32			
	60	-32.1			
Nano-Fe₃O₄	20	-7.853	43.810	0.177	[27]
	25	-9.463			
	30	-10.420			
	35	-10.977			
	40	-11.490			
Activated carbon cocoa shells (ACCS)	20	-6.46	-13.74	-7.43	[38]
	30	-5.80		-7.68	
	40	-5.87		-7.93	
	50	-5.61		-8.19	

Adsorbent	Temperature (°C)	ΔG° (kJ/mol)	ΔH° (kJ/mol)	ΔS° (kJ/mol)	Ref.
Fe NPs	20	-3.35	23.08	0.081	[41]
	30	-4.62			
	40	-6.56			
rGO@nFe/Pd	20	-4.36	17.77	0.075	[43]
	30	-4.59			
	40	-5.88			

Advanced Oxidation Processes

Advanced oxidation processes (AOPs) were first proposed for drinking water treatment in the 1980s and then extensively studied for the treatment of different wastewaters. During the AOP treatment of wastewater, free radicals are generated to remove refractory organic matter, traceable organic pollutants or particular inorganic pollutants, or to increase biodegradability of wastewater as a pretreatment before the next biological treatment [48]. Free radical species (e.g., hydroxyl radicals (•OH), sulfate radicals ($SO_4^{•-}$), singlet oxygen ($^1O_2$), and superoxide radicals ($O_2^{•-}$)) are atoms or molecules that can exist independently and have one or more unpaired electrons [49]. AOPs are characterized by a diversity of radical reactions involving combinations of auxiliary energy sources (e.g., electronic current, ultraviolet-visible (UV-Vis) radiation, ultrasound and γ-radiation) and chemical agents (e.g., hydrogen peroxide (H_2O_2), transition metals, ozone (O_3) and metal oxides). H_2O_2/UV, O_3/UV, O_3/H_2O_2, $O_3/H_2O_2/UV$, Fenton (Fe^{2+}/H_2O_2), photo- and electro-Fenton, chelating agent supported Fenton/photo-Fenton, γ-radiolysis, heterogeneous photooxidation with titanium dioxide (TiO_2/hv) and sonolysis processes are examples of AOPs (Figure 2) [50, 51].

In 1987, Glaze et al. have coined the term AOPs established on the in-situ production of a strong oxidizing agent such as •OH at a adequate concentration to efficiently purify water for water treatment processes carried out at room temperature. •OH is one of the most reactive free radicals and the strongest oxidants (2.80 V) which has a reaction rate of 10^6-10^{10} $M^{-1}s^{-1}$ and can react with various organic molecular groups. The most frequent reactions of •OH with organic pollutants are a substitution of aromatic rings, an addition to unsaturated carbon-carbon bonds, abstraction of the hydrogen atom from the target molecule, or mono-electronic oxidation [52]. In recent years, sulfate radical-based AOPs (SR-AOPs) have been frequently studied to degrade organic pollutants as they overcome some of the shortcomings of •OH radical-based AOPs. $SO_4^{•-}$ is a strong single-electron oxidant with a high oxidation potential (E_0 = 2.5-3.1 V) and a longer life ($t_{1/2}$ = 30–40 μs) allowing excellent electron transfer and contact with target pollutants. In addition, it can selectively react with unsaturated or aromatic compounds over a wide pH range, such as 2-8 [53]. $SO_4^{•-}$ radicals are generated via the activation of peroxymonosulphate (PMS, HSO_5^-) or persulfate (PS, $S_2O_8^{2-}$). The direct reaction of PMS/PS with organic pollutants takes place at a very low rate. Therefore, PMS/PS must be activated to form $SO_4^{•-}$ and can be activated by various methods such as heat, UV, alkali, transition metals (Co^{2+}, Fe^{2+}, Cu^{2+} ve Ag^+) and carbonaceous materials (e.g., activated carbon) [54]. In this section, the different AOPs studied by various researchers for the RIF degradation were reviewed and a summary of these studies reported were presented. Table 4 compares the results of these studies.

AOPs are carried out either in the presence of catalysts (catalytic processes) or in the absence of catalysts (non-catalytic processes). *Catalysts* increase the cavitation effect and the rate of decomposition of organic molecules [55]. Tahvildari et al. [56] used metallic catalysts consisting of zinc (Zn) and copper (Cu) to remove RIF from pharmaceutical wastewaters. Parameters such as total zinc and copper catalyst amount, ratio of catalysts, reaction time, rotation speed, temperature and pH were investigated. As a result, it was found that 96.4% of RIF could be removed from synthetic RIF solutions and real wastewater with 70% zinc and 30% copper at 600 rpm for 120 min, neutral pH and ambient temperature (25 °C). It was concluded that RIF was removed by the oxidation process and adsorption did not occur. It was found that the catalysts could be used repeatedly to remove RIF from wastewater. Madivoli et al. [57] synthesized spherical TiO_2 microspheres by the sol-gel method and investigated for their ability to degrade RIF. When morphology and the size of TiO_2 microspheres were examined by SEM, it was observed that the sizes of the synthesized particles were spherical, varying between 200-2000 nm, and these particles were well dispersed with the absence of aggregates or agglomerates, which was an indicator that the method used was effective for synthesis of microspheres. Degradation of RIF in acidic, neutral and basic medium by microspheres also demonstrated that the antibiotic degradation was pH dependent. The percentage of degradation was higher at pH 12 than at pH 3 and 6.5, and was calculated as 57.6% for pH 3, 62.9% for pH 6.5 and 63.8% for pH 12. However, the degradation rate was higher in acidic medium than in neutral and basic medium. In addition, the existence of H_2O_2 increased the degradation efficiency due to the formation of •OH radicals that help the antibiotic degradation and process followed the first-order reaction pattern.
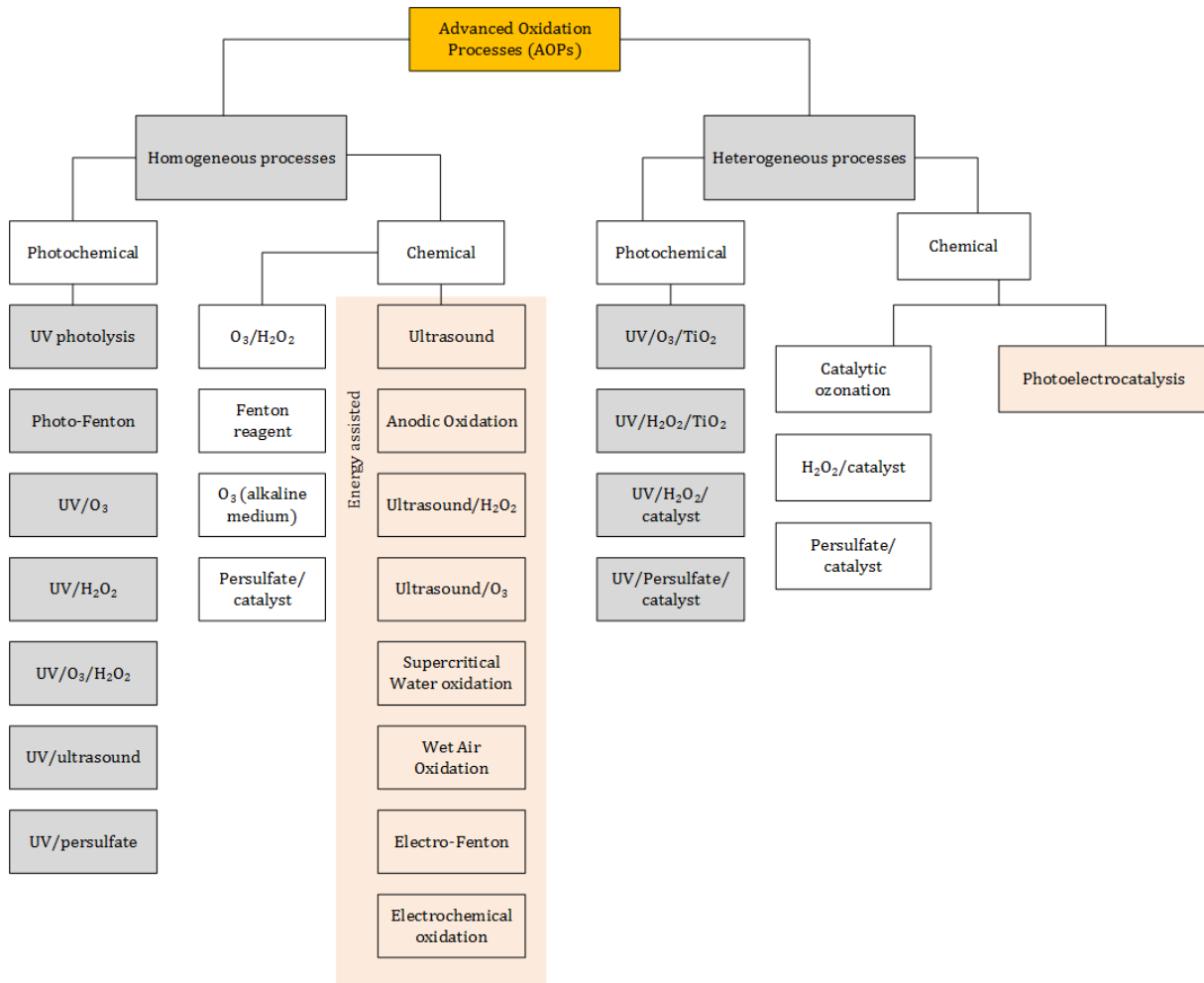
Figure 2. Classification of different treatments based on AOPs [51].

Sonochemical degradation (sonolysis), degradation that is driven or enhanced by sonication, emerged in the 1990s. Ultrasound (US) is sound that exceeds the range of human hearing and has a wide frequency range between 18 kHz and 500 MHz. Ultrasonic propagation with cycles of compression and rarefaction leads to the phenomenon of acoustic cavitation, described as a sonochemical source. Such a large number of cavitation bubbles are also called microreactors as they act as centers of chemical reactions. The cavitation bubbles filled with gas grow and burst extensively under the positive pressure that occurs during the compression cycle of US in water bulk. Meantime, enormous local temperatures (ca. 5000 K) and high pressures (ca. 500 atm), micro jets and shock waves are produced. Then, reactive oxygen species (ROS) are produced by the pyrolysis of water molecules in the collapsing bubbles (hotspots) and oxidizes the substrates in the water. Furthermore, hydrophobic volatile compounds also undergo thermal decomposition in hotspots, and both of the above actions contribute to the degradation of organic pollutants. Theoretically, sonication is capable of degradation a wide range of organic pollutants without added chemicals. Therefore, sonication is frequently considered as a green and safe method for treatment of wastewaters. However, sonolysis of organic pollutants has limited efficiency and consumes significant energy. Sonocatalysis, Sono/Fenton, sonication-ozonation (Sonozonation), sonophotocatalysis (Sono/Photo), sonication-persulfate (Sono/PS), sonoelectrochemical degradation, sonication-microwaves, sonication-hydrodynamic cavitation and sonication-based combinations such as ultrasound-assisted biological processes have attracted great interest to improve removal efficiency and reduce energy consumption (Figure 3) [58].
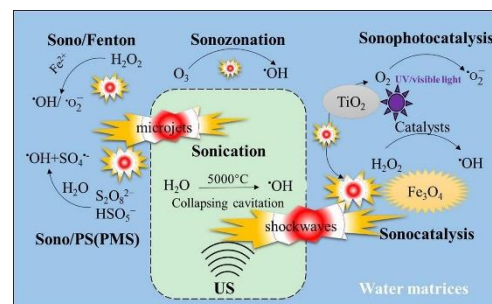

Figure 3. Sonication-involved processes in water matrices (US: ultrasound, PS: peroxydisulfate, PMS: peroxymonosulfate) [58].
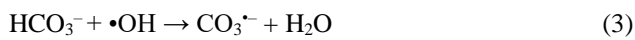
Afroozān Bāzghale and Mohammad-Khāh [59] studied the sonocatalytic RIF removal with nitrogen-doped zinc oxide/graphene oxide hybrid nanocomposite (N:ZnO/GO). This study demonstrated the adequacy of RIF removal (95% at optimum condition) with N:ZnO(0.2 M)/GO in the presence of US. Dumping tests revealed that •OH, $O_2^{•-}$ ve h^+ species play a significant role in the sonocatalytic RIF degradation. For the sonocatalytic degradation of RIF by N:ZnO(0.2 M)/GO, the proposed mechanism was explained as follows: On the one hand, excited electrons in the less positive conduction bond (CB) of N:ZnO move to the more positive valence band (VB) of GO and then it reaches the electrons in the CB, and then the electrons in the CB of N:ZnO and the holes in the VB of GO are combined. On the other hand, electrons aggregated in CB of GO and holes in VB of N-doped ZnO can participate in oxidation and reduction reactions. In fact, electrons in the CB of GO can react with and reduce the absorbed molecular oxygen since these electrons have more negative potential than $O_2/O_2^{•-}$ (-0.3 eV). Moreover, the holes formed in the valence band of ZnO have more positive potential to generate a large number of active OH with high oxidizing ability from water or hydroxyl molecules absorbed from the surface. TOC analysis performed under optimized conditions to investigate the mineralization of the contaminants indicated 80.8% mineralization of RIF after degradation of RIF by N:ZnO(0.2 M)/GO for 60 min. Khataee et al. [60] synthesized ZrO_2-pumice and ZrO_2-tuff nanocomposites by a modified sol-gel method and used them as catalysts for the sonocatalytic degradation of RIF. After characterization studies, it was found that zirconia NPs were immobilized on the surface of pumice and tuff samples without aggregation. BET surface area and pore volume of ZrO_2-pumice and ZrO_2-tuff nanocomposites were determined higher than that of pure pumice and tuff sample (5.87 m^2/g and 1.35 cm^3/g for ZrO_2-pumice and 1.16 m^2/g and 0.27 cm^3/g for ZrO_2-tuff, respectively). It was suggested that these differences can be related to the presence of nano-ZrO_2 particles on the modified samples. The analysis results demonstrated that pH_{PZC} of tuff (7.7) and pumice (7.3) were higher than those of ZrO_2-tuff (6.4) and ZrO_2-pumice (6.5). It was reported that the lower pH_{PZC} of the catalysts than that of pumice and tuff can be due to the low pH_{PZC} (about 5) of the ZrO_2 NPs immobilized on the catalyst surface. It was observed that the degradation efficiency of RIF depended on the initial concentration, dose of catalyst, pH value and ultrasonic power and increased with the addition of enhancers (hydrogen peroxide and potassium persulfate) and different gases (Ar > O_2 > air). It was found that 67.3% COD and 53.8% TOC were removed after 90 min degradation of RIF by the US/ZrO_2-pumice process. Scavenging experiments revealed that •OH radicals were the predominant reactive species responsible for RIF degradation. After five runs, 86.7% and 77.8% of RIF were still degraded by the US/ZrO_2-pumice and US/ZrO_2-tuff treatments, proving the stability of both catalysts.

The IUPAC defines *photocatalysis* as "change in the rate of a chemical reaction or its initiation on exposure to ultraviolet, visible or infrared radiation in the presence of a substance, the photocatalyst that absorbs light quanta and is involved in the chemical transformation of the reaction partners" [61]. Photocatalytic oxidation of organic pollutants was very effective in wastewater treatment due to its advantages such as complete mineralization of substrate and intermediates, operating conditions (ambient temperature and pressure), disposal of solid waste without problems, use of sunlight, visible light or near-UV light for irradiation and cost efficiency. Photocatalysis is a process in which reactive species such as •OH required for the redox are produced upon the catalyst activation by photons. It is considered a very significant technology for solving environmental and energy problems. Two types of photocatalysis are used for the mineralization of organic pollutants in wastewater: homogeneous photocatalysis (e.g., photon-Fenton) and heterogeneous photocatalysis (e.g., solid semiconductors such as WO_3, ZnO and TiO_2) [62]. Heterogeneous photocatalysis refers to a type of catalytic reaction related to various fields including oxidation, hydrogen transfer, dehydrogenation, metal reduction, removal of gaseous pollutants and H_2O detoxification. The classical heterogeneous photocatalysis mechanism usually involves a series of oxidation and reduction reactions on the surface of a semiconductor. The entire process of removing various contaminants can be divided into five steps: (a) Photocatalytic reactions begin with the adsorption of the target substrate onto the photocatalyst surface from the surrounding medium; (b) absorption of light with photon energy greater than the band gap (BG) energy of the photocatalyst and production of photogenerated electron (e^-) - hole (h^+) pairs in bulk phase; (c) migration of e^- and h^+ to the surface of the photocatalyst to participate in the redox reaction and simultaneously, recombination of some photogenerated carriers from the surface and the inside of the photocatalyst; (d) oxidation and reduction of H_2O molecules and O_2 adsorbed on the surface of the photocatalyst to •OH and $O_2^{•-}$ by h^+ in the valence band and e^- in the conduction band, respectively. At the same time, pollutants can be reduced to small molecules (e.g., H_2O and CO_2); and (e) degraded small molecules are desorbed from the interface into the bulk solution and the photoreaction continues [63]. Gao et al. [14] investigated the photocatalytic degradation of RIF on $ZnIn_2S_4$ under visible light irradiation and achieved complete RIF degradation within 90 min. In their studies, they determined that the main ROS was $O_2^{•-}$ and the minor ROS was •OH. The photocatalytic degradation pathway of RIF was proposed. It was stated that the main transformation process for RIF was detachment of the nitrogenous ring via cleavage of the N-N bond, cleavage of nitrogen-bearing heterocycles starting from the C-N bond, demethylation, detachment of acetoxyl group, acetyl and methoxyl. During the 180 min photocatalytic degradation of RIF, 34 kinds of intermediates were detected. Thereinto, it was reported that 21 kinds of intermediates were completely decomposed and then reduced to simpler compounds, and other 13 kinds of products remained as the final product in the reaction mixture after 180 min of photocatalytic reaction.
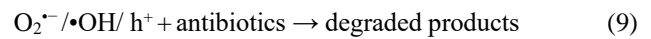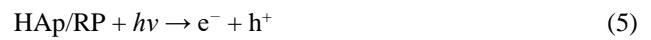
Kais et al. [64] investigated the photocatalytic degradation of RIF in aqueous solution under solar irradiation using ZnO as a photocatalyst. Since the removal of RIF by

adsorption on ZnO or photolysis was weak and did not exceed 4%, the heterogeneous photocatalysis process under solar radiation was applied for RIF removal. ZnO dosage, initial RIF concentration and pH were found to be important factors, and the pH_{PZC} of ZnO was 7.46. With the addition of salts (200 mg/L) to the reaction solution, it was determined that SO_4^{2-} and HCO_3^- negatively affected the process, while Cl^- increased the degradation of RIF. It was suggested that SO_4^{2-} significantly reduced the rate constant following affinity, which causes their fixation on the ZnO surface and the formation of $SO_4^{\bullet-}$ or $\bullet OH$ species according to the reactions in Equations 1-2. In the case of HCO_3^-, the inhibitory effect was explained possibly by the consumption of $\bullet OH$ groups involved in RIF degradation (Equation 3). However, it was stated that the addition of NaCl facilitates the degradation of RIF due to the production of $Cl^{\bullet}$, which has strong oxidizing power (Equation 4). The Langmuir-Hinshelwood model was used in the kinetic study. It was observed that the active species responsible for photocatalytic degradation on ZnO under solar radiation were $\bullet OH$, photon electrons and $O_2^{\bullet-}$, respectively.

$$SO_4^{2-} + h^+ \rightarrow SO_4^{\bullet-} \tag{1}$$

$$SO_4^{2-} + \bullet OH \rightarrow SO_4^{\bullet-} + OH^- \tag{2}$$

$$HCO_3^- + \bullet OH \rightarrow CO_3^{\bullet-} + H_2O \tag{3}$$

$$Cl^- + \bullet OH \rightarrow Cl^{\bullet} + OH^- \tag{4}$$

Soleimani and Nezamzadeh-Ejhieh [65] used a coupled CdS-ZnS system as a photocatalyst for the removal of RIF from an aqueous solution. Cubic ZnS structure and hexagonal CdS structure with a crystallite size of 10 nm were determined from XRD models. It was observed that the coupled ZnS-CdS system had better photocatalytic activity than the single systems, and the best activity was obtained when the moles of CdS were 6 times higher than the ZnS component. When the effects of some scavenging agents were examined to evaluate the importance of the reactive species produced by the coupled ZnS-CdS catalyst for RIF photodegradation, it was concluded that superoxide radicals and photogenerated electrons have a relatively higher role in RIF photodegradation, followed by $\bullet OH$ and finally the photogenerated holes. The mechanism pathway for RIF photodegradation was proposed, and some intermediates (acetic acid, butyramide, formamide, 3-penten-1-ol) was reported in the final mineralization. The reusability of the coupled CdS-ZnS catalyst in RIF photodegradation was investigated in 5 consecutive runs. The degradation activities after 5 runs for the calcination temperature of 100 and 200°C were calculated as 75 and 85%, respectively, confirming that the coupled CdS-ZnS catalyst has relatively high stability for 2 h photodegradation process. Zou et al. [66] synthesized a new and green red phosphorus (5.0 wt%)/hollow hydroxyapatite microsphere (RP (5.0 wt%)/HAp) photocatalyst in RIF degradation. RP particles were immobilized on the surface of hollow HAp microspheres. The BET specific surface

area of RP (5.0 wt%)/HAp (60.3 m²/g) was calculated to be much higher than that of hollow HAp microspheres (44.2 m2/g). The photocatalytic activity of the RP (5.0 wt%)/HAp composite was no significant change even after three runs, thus demonstrating its good recyclability in the degradation of RIF. $O_2^{\bullet-}$, $\bullet OH$, and h^+ were determined to be the dominant active species in the photocatalytic process. Based on the experimental results, a reasonable degradation pathway was suggested and the possible photocatalytic equations were expressed as follows (Equations 5-9):
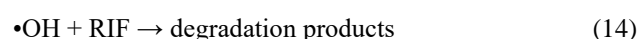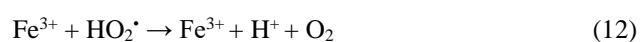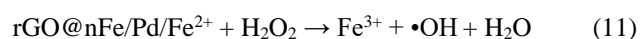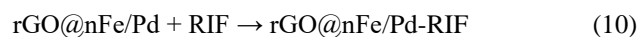
$$HAp/RP + h\nu \rightarrow e^- + h^+ \tag{5}$$

$$e^- (HAp) \rightarrow e^- (RP) \tag{6}$$

$$O_2 + e^- (RP) \rightarrow O_2^{\bullet-} \tag{7}$$

$$H_2O + h^+ (HAp) \rightarrow \bullet OH + H^+ \tag{8}$$

$$O_2^{\bullet-}/\bullet OH/ h^+ + antibiotics \rightarrow degraded\ products \tag{9}$$

In a research, the new photocatalytic TiO_2/Nd/rice husk ash was used for decomposition of RIF. As a result of the experiments, it was determined that the RIF separation efficiency of TiO_2/Nd and TiO_2/Nd/rice husk ash within 90 min under sunlight reached approximately 86% and 75%, respectively. Despite its lower yield, TiO_2/Nd/rice husk ash was chosen to decompose RIF residue in water under sunlight by photocatalytic treatment, since this material has some advantages such as less amount needed and easy recovery. In the RIF removal process, k values were found to fit zero and first-order kinetics more. BET surface areas of nano TiO_2/Nd and TiO_2/Nd/rice husk ash materials were determined as 58.97 and 107 m²/g, respectively. TiO_2/Nd/rice husk ash size was also much larger than the nano TiO_2/Nd particle size. It was suggested that because RIF has bulky molecular structure with many functional groups (-OH, >NH, >C=O etc.), it can easily bond with metals of adsorbents [67].

Electrochemical technologies have become very important around the world due to increasing drinking water supply standards and strict environmental regulations regarding wastewater discharge [68]. Electrochemical oxidation is a process in which organic matter is oxidized and converted or decomposed to non-toxic and harmless substances under the action of an electric current [69]. Electrochemical treatment is interesting processes using an effective, versatile, cost-effective, easy and clean technology for the removal of toxic organic compounds. In electrochemical processes, oxidation takes place on anodes (graphite, TiO_2, Ti-based alloys, Ru or Ir oxides, boron-doped diamond (BDD) etc.) in the presence of an electrolyte [6]. Oxidation of organic pollutants in an electrolytic cell occurs in two different ways: (a) direct electron transfer to the anode and (b) indirect oxidation with heterogeneous ROS formed from water discharge at the anode, such as physisorbed radical $\bullet OH$ or chemisorbed "active oxygen" [70]. Brito et al. used different anodes (boron doped diamond (BDD), PbO_2 and Pt) and cathodes (carbon felt (CF), stainless steel (SS),

graphite (Gr) and titanium (Ti)) for the electrochemical treatment of a synthetic wastewater and different real water matrices contaminated with RIF. The effects on the exchange of applied current density (j) and supporting electrolyte during RIF degradation were investigated. At the end of their studies, it was seen that the process performance increased with an increase in j and better RIF degradation results were obtained by CF and BDD as cathode and anode, respectively. The greater performance of BDD as an anode was attributed to the high •OH production on its surface through water discharge, a prominent feature of this electrode type, which was thought to be inactive. It was noted that since •OH did not strongly adsorbed on the BDD electrode surface, it was relatively free, and was suitable for degradation of RIF and its byproducts. It was reported that the better efficiency of the CF cathode was due to its specific properties, such as high reactive surface area, porosity, high active sites, its ability to respond to the organic pollutant degradation in terms of electro-reduction, and its ability to produce hydrogen peroxide, which is a weak oxidant. 100% color removal was achieved in all applied j, but complete organic matter (chemical oxygen demand (COD)) removal was achieved only at higher j. For a selected cathode, the efficiency of the anode materials followed the trends BDD > PbO$_2$ > Pt, while the efficiency of the cathode for a selected anode material was CF > Ti > SS ≈ Gr. By using Na$_2$CO$_3$, Na$_2$SO$_4$ or NaCl, the production of strong secondary oxidant species was supported. When the BDD/CF electrochemical cell for different real water samples was used, the drug degradation and mineralization were found to be independent of this parameter. •OH was also found to oxidize dissolved organic matter in synthetic wastewater and real water matrices. It was determined that the end-products of RIF degradation were acetic, oxalic, fumaric and maleic acids [71].

Easy to handle and operate, *Fenton systems* can be used to remove micro-pollution caused by residual pharmaceuticals. Fenton oxidation can performed in homogeneous or heterogeneous systems, the former being the most used to date. Homogeneous oxidation with Fenton's reagent occurs from a hydrogen peroxide solution and an iron salt catalyst (iron (II) or iron (III) ions) via a free radical chain reaction generated •OH in acidic medium [6, 72, 73]. Basically, Fenton reactions are based on electron transfer between H$_2$O$_2$ and Fe^{2+}. Both Fe^{2+} and H$_2$O$_2$ do not oxidize target compounds directly, but act as catalysts synergistically in Fenton oxidation. Acting as a predominant reducer of H$_2$O$_2$, metal ions activate H$_2$O$_2$ dissociation to form •OH radicals [74]. Liu et al. [22] synthesized reduced graphene oxide combined with bimetallic iron/palladium nanoparticles (rGO@nFe/Pd) via a green tea extract and used it to remove RIF from aqueous solution. When the composite and Fenton oxidation were combined, the RIF removal increased from 79.9 to 85.7%. The pseudo-second order kinetic model was found to be more fitting to remove RIF by adsorption and Fenton oxidation. Fenton oxidation degradation of RIF by rGO@nFe/Pd was indicated as a surface-controlled reaction (E$_a$: 47.3 kJ/mol). Temperature, H$_2$O$_2$ dose, rGO@nFe/Pd dose, initial RIF concentration and pH were found to affect

RIF removal. The surface area, pore volume and pore size of rGO@nFe/Pd before adsorption was 29.43 m^2/g, 0.128 cm^3/g and 17.36 nm, respectively. After adsorption, the surface area (1.16 m^2/g) and pore volume (0.082 cm^3/g) decreased, while the pore size (281.40 nm) increased significantly, mainly due to the adsorbing of RIF on the surface of rGO@nFe/Pd and to blocking of pores. In addition, after adsorption and Fenton oxidation, the surface area and pore volume of rGO@nFe/Pd increased to 13.76 m^2/g and 0.253 cm^3/g, respectively, while the its pore size decreased to 73.60 nm. This was attributed to the degradation of RIF on rGO@nFe/Pd by •OH, resulting in consequently eluted any pore-blocking materials and changes in the material's surface chemistry causing deactivation of the adsorption sites. Therefore, some RIF was desorbed into the solution. It was suggested that in the initial stages of RIF removal, RIF is mainly removed by adsorption and Fenton oxidation, while in the later removal stages it is mainly removed by Fenton oxidation. The dissolved iron concentration increasing with the reaction in solution was attributed to the continuous iron leaching from rGO@nFe/Pd. In the light of the analysis results and experimental data, it was concluded that the removal mechanism of RIF by rGO@nFe/Pd was a combination of adsorption and Fenton oxidation (Equations 10-14). In addition, it was found that the RIF removal efficiencies of the composite material for river, aquaculture and domestic wastewater were 80.4, 77.9 and 70.2%, respectively. Reusability experiments of rGO@nFe/Pd was shown that even after five cycles, rGO@nFe/Pd still had a relatively high removal efficiency (71.7%).

$$rGO@nFe/Pd + RIF \rightarrow rGO@nFe/Pd\text{-}RIF \qquad (10)$$

$$rGO@nFe/Pd/Fe^{2+} + H_2O_2 \rightarrow Fe^{3+} + \bullet OH + H_2O \qquad (11)$$

$$Fe^{3+} + HO_2{}^\bullet \rightarrow Fe^{3+} + H^+ + O_2 \qquad (12)$$

$$Fe^{3+}\, e^- \,(nPd) \rightarrow Fe^{2+} \qquad (13)$$

$$\bullet OH + RIF \rightarrow \text{degradation products} \qquad (14)$$

Although the treatment of pharmaceuticals widely accomplished by single AOP methods, *hybrid AOP methods* have also received remarkable attention. Compared to single AOP, the removal efficiency of pharmaceuticals has increased due to the increase in the amount of reactive species produced synergistic effect and better mineralization in hybrid systems. To maximize degradation efficiency in these systems, active pharmaceutical ingredients from real or synthetic wastewater are removed either sequentially or simultaneously [75]. Duarte et al. [15] compared the performance of Fenton reaction, electrochemical treatment and combined treatment processes for the removal of synthetic wastewater containing RIF. Regarding the studied electrode materials, it was determined that the RIF degradation efficiency decreased in the order of BDD >> Ti/Pt > Ti/Ru$_{0.3}$Ti$_{0.7}$O$_2$ (DSA, Dimensionally stable anode). Higher efficiency of BDD was attributed to
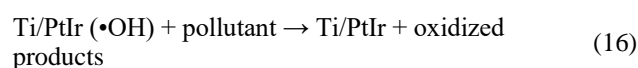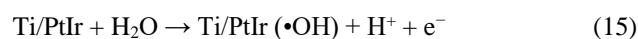
the high amount of free hydroxyl radicals produced by BDD, which promoted significantly degradation/mineralization of organic substrates more efficiently than the $RuO_{(x+1)}$ and $PtO_{(x+1)}$ species formed on Ti/Pt and $Ti/Ru_{0.3}Ti_{0.7}O_2$ surfaces. It was also suggested that persulfate could be produced electrochemically at the BDD anode, which contributed to the pollutant oxidation. When the results from removal of RIF-containing synthetic wastewater by electrooxidation were compared with the Fenton reaction, the Fenton reaction was found to be efficient because at 20 mmol/L H_2O_2 concentration, RIF absorbance and COD were reduced by approximately 91% and 79%, respectively. When BDD electrolysis was studied by applying 90mA/cm^2, approximately 95% of RIF absorbance and 81% of COD were removed. However, it took a shorter time (40 min) for effluent treatment by Fenton reaction compared to BDD-electrolysis. Both the electrochemical process and the Fenton reaction did not fully mineralize the RIF. Under the optimum conditions of the electrochemical process and the Fenton reaction, 19 and 21% of the COD remained in solution, respectively, as resistant intermediates were likely formed during the processes. The combined process (electrochemical treatment + Fenton reaction) was used to increase the efficiency of RIF removal in the purification. The results clearly showed that no significant improvement was made when both technologies were combined. However, a remarkable increase in reaction efficiency was observed in the use of BDD when H_2O_2 was added to the electrochemical process.

Stets et al. [76] evaluated the degradation efficiency of photo-assisted AOPs (UV/TiO_2, UV/ZnO, homogeneous and heterogeneous Fenton and photo-Fenton processes) using RIF as the target pollutant. As a result of the experiments, it was found that approximately 95% of RIF were removed in 60 min by UV-A TiO_2-photocatalysis under optimized conditions, while the ZnO-assisted photocatalytic degradation was lower than that of TiO_2, probably due to the lower specific surface area of ZnO (5 m^2/g) and its tendency to agglomerate larger. The low-cost UV-A homogeneous photo-Fenton treatment removed 80% of the RIF in 60 min. The photo-Fenton process using iron-immobilized in chitosan beads showed lower degradation efficiency (50%), probably due to the lower iron availability on the catalyst surface. The results showed that the RIF degradation process was mainly affected by h$^+$, as demonstrated by a reduction of the degradation rate to 30% in the presence of sodium oxalate. RIF reactivity towards h$^+$ was stated to be consistent with its high adsorption (15%) to the photocatalyst surface and abundance of donating electron pairs.
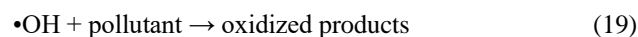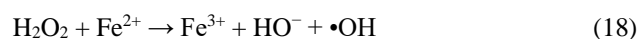
Mukimin et al. [77] aimed to propose a new solution for antibiotic RIF degradation via three electrocatalytic based mechanisms, namely electrochemical advanced oxidation (EAOP), electrochemical Fenton reagent (EFRP) and electrochemical flotation processes (EFP), while producing peroxide as an intermediate. Performance of process was evaluated with COD removal, UV–VIS absorbance spectra and time-of-flight mass spectrometry analysis (TOF-MS).

As a result, RIF was efficiently degraded. Complete mineralization was achieved as indicated by 100% COD removal as well as the disappearance of the UV-VIS absorbance spectrum peaks at λ 470, 340 and 240 nm of the treated wastewater. In addition, this result was supported by the TOF-MS analysis results showing the absence of chromatogram peaks in m/z 821, m/z 759, m/z 700 and m/z 144. It was concluded that COD removal was probably achieved through three mechanisms (EAOP, EFRP and EFP), as in the equations below (Equations 15-21):
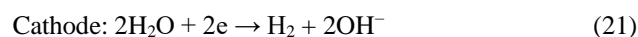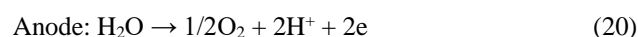
EAOP:

$$Ti/PtIr + H_2O \rightarrow Ti/PtIr\ (\bullet OH) + H^+ + e^- \qquad (15)$$

$$Ti/PtIr\ (\bullet OH) + pollutant \rightarrow Ti/PtIr + oxidized\ products \qquad (16)$$

$$2H^+ + O_2 + 2e^- \rightarrow H_2O_2 \qquad (17)$$

EFRP

$$H_2O_2 + Fe^{2+} \rightarrow Fe^{3+} + HO^- + \bullet OH \qquad (18)$$

$$\bullet OH + pollutant \rightarrow oxidized\ products \qquad (19)$$

EFP

$$Anode: H_2O \rightarrow 1/2O_2 + 2H^+ + 2e \qquad (20)$$

$$Cathode: 2H_2O + 2e \rightarrow H_2 + 2OH^- \qquad (21)$$

From the above studies, it is seen that photocatalysis, electrochemical, US-assisted AOPs, Fenton process and heterogeneous catalysis was generally used for RIF degradation. Typically, these AOPs studies included the effect of operational parameters, kinetics, mineralization measurements (TOC or COD), mechanism of degradation, transformation products, quenching tests to identify the predominant reactive species, and reusability tests to determine catalyst stability if used. Existing data suggest that these AOPs have great potential for the removal of resistant organic pollutants such as RIF from wastewaters. Although good removal efficiencies was observed using AOPs, in most of the studies RIF could not be completely degraded and turned into transformation products.

Other Technologies

In addition to adsorption and AOP methods, other technologies applied for RIF removal in the literature are reviewed and a summary of the researches performed is presented in this section. Membrane-based processes have attracted much attention for water treatment due to their properties such as high efficiency, environmental friendliness, lower cost, lower footprint, scalability and simplicity. Actually, membranes play a significant role in the challenges of water treatment [78]. Arefi-Oskoui et al. [79] used the nanocomposite of MoS_2 nanosheets and oxidized multi-walled carbon nanotubes (MoS_2/O-MWCNTs) as a nano additive for the improvement of polyethersulfone (PES) polymeric membrane. They

157

investigated the effective removal of RIF by 0.75 wt% MoS_2/O-MWCNTs/PES to evaluate the potential of developed membranes in the treatment of different wastewaters using membrane-based processes. A uniform flat surface without any agglomeration was observed for all blended membranes. For bare and blended membranes, asymmetrical structure was observed with small pores in the uplayer and finger-like pores in the sublayer, indicating that the membrane formation mechanism did not change in the presence of nanoadditive in the dope solution. When the homogeneous distribution of MoS_2/O-MWCNTs nanocomposite in the blended membrane matrix was examined, it was revealed that the average surface roughness, porosity, hydrophilicity and average pore size increased by blending the optimum MoS_2/O-MWCNTs amount (0.75 wt%). The modified blended membrane (0.75 wt% MoS_2/O-MWCNTs/PES membrane) showed better permeability (flux: 192.2 L/m^2.h) and better antifouling (FRR: 60.8%) compared to bare PES membrane (flux: 128.1 L/m^2.h and FRR: 50.0%). As a result, the 0.75 wt% MoS_2/O-MWCNTs/PES membrane exhibited permeability of 64.1 L/m^2.h.bar and 97.5% removal for RIF.

MBBRs (Moving Bed Biofilm Reactors) are based on biofilms grown on small plastic carriers (1-4 cm in diameter) suspended and stirred in a reactor. In this way, MBBRs offer the advantages of biofilm reactors while being as robust in design as activated sludge treatment.

MBBRs have been recognized as compact and robust reactors for wastewater treatment in terms of increasing nitrification. Recently, it was proven by many studies that different biofilm technologies can remove micropollutants. Among these biofilm technologies, MBBRs have turned out to be a promising solution for the removal of micropollutants such as pharmaceuticals [80]. Li et al. [81] investigated the removal of some antibiotics (including RIF) using a MBBR and evaluated the effects of antibiotics on the organic matter removal, changes in ARGs and the abundance of antibiotic resistant bacteria (ARB), and changes in the bacterial community in reactors caused by antibiotics. It was concluded that sub-μg/L-sub-mg/L concentrations of antibiotics did not have a important effect on TOC removal. It was also reported that the relative abundance of ARGs and ARBs in the MBBR biofilm is increased due to the selective pressure of antibiotics. In addition, it was determined that antibiotics reduced the diversity of the biofilm bacterial community and changed the structure of bacterial community. It was suggested that these results will provide an empirical basis for the development of suitable practices for aquaculture and that disinfection and advanced oxidation should be applied to remove antibiotics, ARGs and ARB from mariculture wastewater.

Table 4. Comparison of different AOPs used by various researchers for degradation of RIF.

Process type	Conditions	Removal (%)	Ref.
$ZnIn_2S_4$/visible light irradiation	RIF: 10 mg/L, $ZnIn_2S_4$: 50 mg/L, light intensity: 50 mW/cm^2 (100 W iodine-gallium lamp), 90 min	100	[14]
Electrochemical process (BDD anode)	RIF: 0.2 g/L, Na_2SO_4: 0.5 M, current density: 90 mA/cm^2, pH: 3, 30 °C, 3 h	95 81 (COD)	[15]
Fenton reaction	RIF: 0.2 g/L, Fe^{2+}: 0.1 mM, H_2O_2: 20 mM, pH: 3, 15 min	91 79 (COD)	[15]
Electrochemical process + Fenton reaction	RIF: 0.2 g/L, Fe^{2+}: 0.1 mM, H_2O_2: 5 mM, Na_2SO_4: 0.5 M, current density: 30 mA/cm^2, pH: 3, 3 h	45 (BDD) 46 (Ti/Pt) 43 (Ti/$Ru_{0.3}Ti_{0.7}O_2$) (COD)	[15]
rGO@nFe/Pd	RIF: 20 mg/L, rGO@nFe/Pd: 0.2 g/L, pH: 6.14, 30 °C	79.9	[22]
rGO@nFe/Pd + Fenton	RIF: 50 mg/L, rGO@nFe/Pd: 0.2 g/L, H_2O_2: 74 mM, pH:6.14, 30 °C	85.7	[22]
Metallic catalysts (Zn/Cu)	RIF: 40 ppm, Zn/Cu (%): 70/30, 600 rpm, neutral pH, 25 °C, 120 min	96.4	[56]
US/(N:ZnO/GO)	RIF: 30 mg/L, catalyst: 0.1 g, frequency: 50 KHz, US power: 400 W, natural pH, 25 ± 3 °C, 60 min	95	[59]
US/ZrO_2-pumice	RIF: 20 mg/L, catalyst: 1.5 g/L, frequency: 40 KHz, US power: 300 W, natural pH, 25 ± 3 °C, 90 min	95	[60]
US/ZrO_2-tuff	RIF: 20 mg/L, catalyst: 1.5 g/L, frequency: 40 KHz, US power: 300 W, natural pH, 25 ± 3 °C, 90 min	83	[60]
CdS-ZnS/solar irridation	RIF: 8 mg/L, CdS-ZnS: 0.5 g/L, pH: 2, 120 min	98	[65]
RP (5.0 wt%)/HAp composite	RIF: 10 mg/L, catalyst: 1.0 g/L, pH: 6, 20 min, 300 W Xe lamp	100	[66]

Process type	Conditions	Removal (%)	Ref.
$ZnIn_2S_4$/visible light irradiation	RIF: 10 mg/L, $ZnIn_2S_4$: 50 mg/L, light intensity: 50 mW/cm^2 (100 W iodine-gallium lamp), 90 min	100	[14]
Electrochemical process (BDD anode)	RIF: 0.2 g/L, Na_2SO_4: 0.5 M, current density: 90 mA/cm^2, pH: 3, 30 °C, 3 h	95 81 (COD)	[15]
Fenton reaction	RIF: 0.2 g/L, Fe^{2+}: 0.1 mM, H_2O_2: 20 mM, pH: 3, 15 min	91 79 (COD)	[15]
Electrochemical process + Fenton reaction	RIF: 0.2 g/L, Fe^{2+}: 0.1 mM, H_2O_2: 5 mM, Na_2SO_4: 0.5 M, current density: 30 mA/cm^2, pH: 3, 3 h	45 (BDD) 46 (Ti/Pt) 43 ($Ti/Ru_{0.3}Ti_{0.7}O_2$) (COD)	[15]
BDD/CF cell	RIF: 0.2 mM, Na_2SO_4: 50 mM, current density: 50 mA/cm^2, 6 h	100	[71]
TiO_2/UV-A photocatalysis	RIF: 10 mg/L, TiO_2: 0.5 g/L, radiation: 125 W, pH: 6, 25 ± 1 °C, 60 min	95	[76]
Homogeneous UV-A photo-Fenton process	RIF: 10 mg/L, Fe^{2+}: 15 mg/L, H_2O_2: 150 mg/L, pH: 3, 25 ± 1 °C, 60 min	80	[76]
Heterogeneous UV-A photo-Fenton process	RIF: 10 mg/L, Fe-immobilized chitosan: 10 g, H_2O_2: 150 mg/L, pH: 6, 25 ± 1 °C, 60 min	50	[76]

Conclusions

This review highlighted the treatment processes used for the removal of RIF from aqueous matrices, and recommendations for future studies were outlined. AOPs, adsorption and several other treatment processes were applied for the removal of RIF. Different adsorbents were investigated for RIF adsorption and almost all studied adsorbents effectively removed RIF. Although the adsorption process is effective, no information could be found in the researches about cost of process and the disposal of the used adsorbent, which can be considered as the hazardous waste that is the main drawbacks of adsorption. The AOPs were the other most investigated course of treatment for the removal of RIF. Except for the heterogeneous UV-A photo-Fenton process, all AOPs were successfully performed for RIF degradation. Although the current AOPs used for the degradation of RIF have shown very good efficiencies, their transformation products and high costs limited their large-scale application in wastewater treatment plants. In addition, sulfate radical-based AOPs, which have attracted the attention of researchers in recent years, were not used for the degradation of RIF. A membrane-based process was also used for RIF removal and was successful. However, MBBR biofilm has not been a successful process for RIF removal, and the application of disinfection and AOPs to remove antibiotics, ARGs and ARB from marine culture wastewater was suggested by researchers.

As a result, it can be said that AOPs and adsorption process can be the most suitable processes for RIF removal. Although these processes are effective, the necessity of minimizing or eliminating some of their disadvantages is critical. Furthermore, since the matrix of real wastewater samples is more complex compared to synthetic wastewater samples, further researches should be performed using real wastewater samples for successful RIF removal. In addition, more research on the toxicity of RIF should be performed. The number of studies on the removal of RIF can be increased and different removal methods can be tried. From this review, it can be concluded that RIF removal has recently attracted the attention of many researchers and is an important for the environment and human health.

Ethics committee approval and conflict of interest statement

"There is no need to obtain permission from the ethics committee for the article prepared"

"There is no conflict of interest with any person / institution in the article prepared"

References

[1] S.N. Oba, J. O. Ighalo, C.O. Aniagor, and C.A. Igwegbe, "Removal of ibuprofen from aqueous media by adsorption: A comprehensive review," *Science of The Total Environment*, Vol. 780, p. 146608, 2021. https://doi.org/10.1016/j.scitotenv.2021.146608.

[2] T. Deblonde, C. Cossu-Leguille, and P. Hartemann, "Emerging pollutants in wastewater: A review of the literature," *International Journal of Hygiene and Environmental Health*, Vol. 214 (6), pp. 442-448, 2011. https://doi.org/10.1016/j.ijheh.2011.08.002.

[3] M. Patel, R. Kumar, K. Kishor, T. Mlsna, C. U. Pittman, and D. Mohan, "Pharmaceuticals of Emerging Concern in Aquatic Systems: Chemistry, Occurrence, Effects, and Removal Methods," *Chemical Reviews*, Vol. 119 (6), pp. 3510-3673, 2019. 10.1021/acs.chemrev.8b00299.

[4] I. Michael, L. Rizzo, C.S. McArdell, C.M. Manaia, C. Merlin, T. Schwartz, C. Dagot, D. Fatta-Kassinos, "Urban wastewater treatment plants as hotspots for the release of antibiotics in the environment: A review,"

Water Research, Vol. 47 (3), pp. 957-995, 2013. https://doi.org/10.1016/j.watres.2012.11.027.

[5] K. Kümmerer, "Antibiotics in the aquatic environment – A review – Part I," Chemosphere, Vol. 75, no. 4, pp. 417-434, 2009. https://doi.org/10.1016/j.chemosphere.2008.11.086.

[6] V. Homem and L. Santos, "Degradation and removal methods of antibiotics from aqueous matrices – A review," *Journal of Environmental Management*, Vol. 92 (10), pp. 2304-2347, 2011. https://doi.org/10.1016/j.jenvman.2011.05.023.

[7] E.A. Campbell, N. Korzheva, A. Mustaev, K. Murakami, S. Nair, A. Goldfarb, S.A. Darst, "Structural Mechanism for Rifampicin Inhibition of Bacterial RNA Polymerase," *Cell*, Vol. 104 (6), pp. 901-912, 2001. https://doi.org/10.1016/S0092-8674(01)00286-0.

[8] R. Shokri and M. Amjadi, "Boron and nitrogen co-doped carbon dots as a chemiluminescence probe for sensitive assay of rifampicin," *Journal of Photochemistry and Photobiology A: Chemistry*, Vol. 425, p. 113694, 2022. https://doi.org/10.1016/j.jphotochem.2021.113694.

[9] H. Soni and J. Malik, "Rifampicin as Potent Inhibitor of COVID -19 Main Protease: In-Silico Docking Approach," *Saudi Journal of Medical and Pharmaceutical Sciences*, Vol. 6, pp. 588-593, 2020. 10.36348/sjmps.2020.v06i09.001.

[10] M. Shafaati, M. Miralinaghi, R.H.S.M. Shirazi, and E. Moniri, "The use of chitosan/Fe3O4 grafted graphene oxide for effective adsorption of rifampicin from water samples," *Research on Chemical Intermediates*, Vol. 46 (12), pp. 5231-5254, 2020. 10.1007/s11164-020-04259-9.

[11] S. Rastgar and S. Shahrokhian, "Nickel hydroxide nanoparticles-reduced graphene oxide nanosheets film: Layer-by-layer electrochemical preparation, characterization and rifampicin sensory application," *Talanta*, Vol. 119, pp. 156-163, 2014. https://doi.org/10.1016/j.talanta.2013.10.047.

[12] A. Tupin, M. Gualtieri, F. Roquet-Banères, Z. Morichaud, K. Brodolin, and J.-P. Leonetti, "Resistance to rifampicin: at the crossroads between ecological, genomic and medical concerns," *International Journal of Antimicrobial Agents*, Vol. 35 (6), pp. 519-523, 2010. https://doi.org/10.1016/j.ijantimicag.2009.12.017.

[13] N. Forrest Graeme and K. Tamura, "Rifampin Combination Therapy for Nonmycobacterial Infections," *Clinical Microbiology Reviews*, Vol. 23 (1), pp. 14-34, 2010, 10.1128/CMR.00034-09.

[14] B. Gao, S. Dong, J. Liu, L. Liu, Q. Feng, N. Tan, T. Liu, L. Bo, L. Wang, "Identification of intermediates and transformation pathways derived from photocatalytic degradation of five antibiotics on ZnIn$_2$S$_4$," *Chemical Engineering Journal*, Vol. 304, pp. 826-840, 2016. https://doi.org/10.1016/j.cej.2016.07.029.

[15] J.L.d.S. Duarte, A.M.S. Solano, M.L.P.M. Arguelho, J. Tonholo, C.A. Martínez-Huitle, and C.L.d.P.e.S. Zanta, "Evaluation of treatment of effluents contaminated with rifampicin by Fenton, electrochemical and associated processes," *Journal of Water Process Engineering*, Vol. 22, pp. 250-257, 2018. https://doi.org/10.1016/j.jwpe.2018.02.012.

[16] W. H. Organization, "World Health Organization model list of essential medicines: 21st list 2019," World Health Organization, 2019.

[17] E. Grotz, E. Bernabeu, M. Pappalardo, D.A. Chiappetta, and M.A. Moretton, "Nanoscale Kolliphor® HS 15 micelles to minimize rifampicin self-aggregation in aqueous media," *Journal of Drug Delivery Science and Technology*, Vol. 41, pp. 1-6, 2017. https://doi.org/10.1016/j.jddst.2017.06.009.

[18] C. Becker, J.B. Dressman, H.E. Junginger, S. Kopp, K.K. Midha, V.P. Shah, S. Stavchansky, D.M. Barends, "Biowaiver monographs for immediate release solid oral dosage forms: Rifampicin," *Journal of Pharmaceutical Sciences*, https://doi.org/10.1002/jps.21624 Vol. 98 (7), pp. 2252-2267, 2009. https://doi.org/10.1002/jps.21624.

[19] K. Hao, S. Suryoprabowo, S. Song, H. Kuang, and L. Liu, "Rapid detection of rifampicin in fish using immunochromatographic strips," *Food and Agricultural Immunology*, Vol. 31 (1), pp. 700-710, 2020. 10.1080/09540105.2020.1753017.

[20] A.U. Khan, F. Shah, R.A. Khan, B. Ismail, A.M. Khan, and H. Muhammad, "Preconcentration of rifampicin prior to its efficient spectroscopic determination in the wastewater samples based on a nonionic surfactant," *Turkish Journal of Chemistry*, Vol. 45 (4), pp. 1201-1209, 2021. 10.3906/kim-2102-28.

[21] D.C. Henrique, D.U. Quintela, A.H. Ide, A. Erto, J.L.d.S. Duarte, and L. Meili, "Calcined Mytella falcata shells as alternative adsorbent for efficient removal of rifampicin antibiotic from aqueous solutions," *Journal of Environmental Chemical Engineering*, Vol. 8 (3), p. 103782, 2020. https://doi.org/10.1016/j.jece.2020.103782.

[22] L. Liu, Q. Xu, G. Owens, and Z. Chen, "Fenton-oxidation of rifampicin via a green synthesized rGO@nFe/Pd nanocomposite," *Journal of Hazardous Materials*, Vol. 402, p. 123544, 2021. https://doi.org/10.1016/j.jhazmat.2020.123544.

[23] X. Hu, K. He, and Q. Zhou, "Occurrence, accumulation, attenuation and priority of typical antibiotics in sediments based on long-term field and modeling studies," *Journal of Hazardous Materials*, Vol. 225-226, pp. 91-98, 2012. https://doi.org/10.1016/j.jhazmat.2012.04.062.

[24] J. Du, H. Zhao, and J. Chen, "[Simultaneous determination of 23-antibiotics in mariculture water using solid-phase extraction and high performance liquid chromatography-tandem mass spectrometry]," (in chi), *Se pu = Chinese journal of chromatography*, Vol. 33 (4), pp. 348-53, 2015. 10.3724/sp.j.1123.2014.09028.

[25] H. Thuy and T. Loan, "Antibiotic residues from shrimp farming in coastal wetland," *Natural Resources and Environment*, Vol. 2 (2012), pp. 61-63, 2012.

[26] A. Rico, R. Jacobs, P. J. Van den Brink, and A. Tello, "A probabilistic approach to assess antibiotic resistance development risks in environmental compartments and its application to an intensive aquaculture production scenario," *Environmental Pollution*, Vol. 231, pp. 918-928, 2017. https://doi.org/10.1016/j.envpol.2017.08.079.

[27] W. Cai, X. Weng, and Z. Chen, "Highly efficient removal of antibiotic rifampicin from aqueous solution using green synthesis of recyclable nano-Fe$_3$O$_4$," *Environmental Pollution*, Vol. 247, pp. 839-846, 2019. https://doi.org/10.1016/j.envpol.2019.01.108.

[28] J.-J. Huang, H-Y. Hu, S-Q. Lu, Y. Li, F. Tang, Y. Lu, B. Wei, "Monitoring and evaluation of antibiotic-resistant bacteria at a municipal wastewater treatment plant in China," *Environment International*, Vol. 42, pp. 31-36, 2012. https://doi.org/10.1016/j.envint.2011.03.001.

[29] J. Cao, Y. Mi, C. Shi, Y. Bian, C. Huang, Z. Ye, L. Liu, L. Miao, "First-line anti-tuberculosis drugs induce hepatotoxicity: A novel mechanism based on a urinary metabolomics platform," *Biochemical and Biophysical Research Communications*, Vol. 497 (2), pp. 485-491, 2018. https://doi.org/10.1016/j.bbrc.2018.02.030.

[30] M. Combrink, D.T. Loots, and I. du Preez, "Metabolomics describes previously unknown toxicity mechanisms of isoniazid and rifampicin," *Toxicology Letters*, Vol. 322, pp. 104-110, 2020. https://doi.org/10.1016/j.toxlet.2020.01.018.

[31] Y. Liao, S.Q. Peng, X.Z. Yan, H.B. Chen, and L.S. Zhang, "[Metabonomic profile of urine from rats administrated with different treatment period of rifampin]," (in chi), Zhongguo yi xue ke xue yuan xue bao. *Acta Academiae Medicinae Sinicae*, Vol. 30 (6), pp. 696-702, 2008.

[32] R.M. Jasmer, J.J. Saukkonen, H.M. Blumberg, C.L. Daley, J. Bernardo, E. Vittinghoff, M.D. King, L.M. Kawamura, P.C. Hopewell, "Short-Course Rifampin and Pyrazinamide Compared with Isoniazid for Latent Tuberculosis Infection: A Multicenter Clinical Trial," *Annals of Internal Medicine*, Vol. 137 (8), pp. 640-647, 2002, 10.7326/0003-4819-137-8-200210150-00007.

[33] B.S. Rathi and P.S. Kumar, "Application of adsorption process for effective removal of emerging contaminants from water and wastewater,"

Environmental Pollution, Vol. 280, p. 116995, 2021. https://doi.org/10.1016/j.envpol.2021.116995.

[34] C.P. Silva, G. Jaria, M. Otero, V.I. Esteves, and V. Calisto, "Waste-based alternative adsorbents for the remediation of pharmaceutical contaminated waters: Has a step forward already been taken?," *Bioresource Technology*, Vol. 250, pp. 888-901, 2018. https://doi.org/10.1016/j.biortech.2017.11.102.

[35] J. Ouyang, L. Zhou, Z. Liu, J.Y.Y. Heng, and W. Chen, "Biomass-derived activated carbons for the removal of pharmaceutical mircopollutants from wastewater: A review," *Separation and Purification Technology*, Vol. 253, p. 117536, 2020. https://doi.org/10.1016/j.seppur.2020.117536.

[36] M.J. Ahmed, "Adsorption of non-steroidal anti-inflammatory drugs from aqueous solution using activated carbons: Review," *Journal of Environmental Management*, Vol. 190, pp. 274-282, 2017. https://doi.org/10.1016/j.jenvman.2016.12.073.

[37] M. Erdem, R. Orhan, M. Şahin, and E. Aydın, "Preparation and Characterization of a Novel Activated Carbon from Vine Shoots by ZnCl$_2$ Activation and Investigation of Its Rifampicine Removal Capability," *Water, Air, & Soil Pollution*, Vol. 227 (7), p. 226, 2016. 10.1007/s11270-016-2929-5.

[38] H. Kais, N. Yeddou Mezenner, and M. Trari, "Biosorption of rifampicin from wastewater using cocoa shells product," *Separation Science and Technology*, Vol. 55 (11), pp. 1984-1993, 2020. 10.1080/01496395.2019.1623255.

[39] L. Rusu, C-G. Grigoraş, E.M. Suceveanu, A-I. Simion, A.V. Dediu Botezatu, B. Istrate, I. Doroftei, "Eco-Friendly Biosorbents Based on Microbial Biomass and Natural Polymers: Synthesis, Characterization and Application for the Removal of Drugs and Dyes from Aqueous Solutions," *Materials*, Vol. 14 (17), 2021. 10.3390/ma14174810.

[40] W.-x. Zhang, "Nanoscale Iron Particles for Environmental Remediation: An Overview," *Journal of Nanoparticle Research*, Vol. 5 (3), pp. 323-332, 2003, 10.1023/A:1025520116015.

[41] Z. Lin, X. Weng, G. Owens, and Z. Chen, "Simultaneous removal of Pb(II) and rifampicin from wastewater by iron nanoparticles synthesized by a tea extract," *Journal of Cleaner Production*, Vol. 242, p. 118476, 2020. https://doi.org/10.1016/j.jclepro.2019.118476.

[42] Q. Xu, W. Li, X. Weng, G. Owens, and Z. Chen, "Mechanism and impact of synthesis conditions on the one-step green synthesis of hybrid RGO@Fe/Pd nanoparticles," *Science of The Total Environment*, Vol. 710, p. 136308, 2020/03/25/ 2020. https://doi.org/10.1016/j.scitotenv.2019.136308.

[43] Q. Xu, G. Owens, and Z. Chen, "Adsorption and catalytic reduction of rifampicin in wastewaters using

hybrid rGO@Fe/Pd nanoparticles," *Journal of Cleaner Production*, Vol. 264, p. 121617, 2020. https://doi.org/10.1016/j.jclepro.2020.121617.

[44] C. Xue, W. Cai, X. Weng, G. Owens, and Z. Chen, "A one step synthesis of hybrid Fe/Ni-rGO using green tea extract for the removal of mixed contaminants," *Chemosphere*, Vol. 284, p. 131369, 2021. https://doi.org/10.1016/j.chemosphere.2021.131369.

[45] A.R. Abbasi and M. Rizvandi, "Influence of the ultrasound-assisted synthesis of Cu–BTC metal–organic frameworks nanoparticles on uptake and release properties of rifampicin," *Ultrasonics Sonochemistry*, Vol. 40, pp. 465-471, 2018. https://doi.org/10.1016/j.ultsonch.2017.07.041.

[46] A.F.d. Silva, J.L.d.S. Duarte, and L. Meili, "Different routes for MgFe/LDH synthesis and application to remove pollutants of emerging concern," *Separation and Purification Technology*, Vol. 264, p. 118353, 2021. https://doi.org/10.1016/j.seppur.2021.118353.

[47] A. Hussain, W.A. Mahdi, S. Alshehri, S.I. Bukhari, and M.A. Almaniea, "Application of Green Nanoemulsion for Elimination of Rifampicin from a Bulk Aqueous Solution," *International Journal of Environmental Research and Public Health*, Vol. 18 (11), 2021. 10.3390/ijerph18115835.

[48] Y. Deng and R. Zhao, "Advanced Oxidation Processes (AOPs) in Wastewater Treatment," *Current Pollution Reports*, Vol. 1 (3), pp. 167-176, 2015. 10.1007/s40726-015-0015-z.

[49] J.L. Wang and L.J. Xu, "Advanced Oxidation Processes for Wastewater Treatment: Formation of Hydroxyl Radical and Application," *Critical Reviews in Environmental Science and Technology*, Vol. 42 (3), pp. 251-325, 2012. 10.1080/10643389.2010.507698.

[50] K. Ikehata, N. Jodeiri Naghashkar, and M. Gamal El-Din, "Degradation of Aqueous Pharmaceuticals by Ozonation and Advanced Oxidation Processes: A Review," *Ozone: Science & Engineering*, Vol. 28 (6), pp. 353-414, 2006. 10.1080/01919510600985937.

[51] C. Amor, L. Marchão, M.S. Lucas, and J.A. Peres, "Application of Advanced Oxidation Processes for the Treatment of Recalcitrant Agro-Industrial Wastewater: A Review," *Water*, Vol. 11 (2), 2019. 10.3390/w11020205.

[52] M. Trojanowicz, A. Bojanowska-Czajka, I. Bartosiewicz, and K. Kulisa, "Advanced Oxidation/Reduction Processes treatment for aqueous perfluorooctanoate (PFOA) and perfluorooctanesulfonate (PFOS) – A review of recent advances," *Chemical Engineering Journal*, Vol. 336, pp. 170-199, 2018. https://doi.org/10.1016/j.cej.2017.10.153.

[53] Y. Gao, P. Champagne, D. Blair, O. He, and T. Song, "Activated persulfate by iron-based materials used for refractory organics degradation: a review," *Water Science and Technology*, Vol. 81 (5), pp. 853-875, 2020. 10.2166/wst.2020.190.

[54] S. Guerra-Rodríguez, E. Rodríguez, D.N. Singh, and J. Rodríguez-Chueca, "Assessment of Sulfate Radical-Based Advanced Oxidation Processes for Water and Wastewater Treatment: A Review," *Water*, Vol. 10 (12), 2018. 10.3390/w10121828.

[55] J.O. Ighalo, C.A. Igwegbe, C.O. Aniagor, and S.N. Oba, "A review of methods for the removal of penicillins from water," *Journal of Water Process Engineering*, Vol. 39, p. 101886, 2021. https://doi.org/10.1016/j.jwpe.2020.101886.

[56] K. Tahvildari and T. Bigdeli, "Treatment of pharmaceutical wastewater containing antibiotic with oxidation processes by metallic catalysts," *Biointerface Research in Applied Chemistry*, Vol. 9 (2), pp. 3853 - 3859, 2019. 10.33263/BRIAC92.853859.

[57] E.S. Madivoli, P. G. Kareru, D.S. Makhanu, K. S. Wandera, E.G. Maina, S.I. Wanakai, P.K. Kimani, "Synthesis of spherical titanium dioxide microspheres and its application to degrade rifampicin," *Environmental Nanotechnology, Monitoring & Management*, Vol. 14, p. 100327, 2020. https://doi.org/10.1016/j.enmm.2020.100327.

[58] P. Liu, Z. Wu, A.V. Abramova, and G. Cravotto, "Sonochemical processes for the degradation of antibiotics in aqueous solutions: A review," *Ultrasonics Sonochemistry*, Vol. 74, p. 105566, 2021, https://doi.org/10.1016/j.ultsonch.2021.105566.

[59] Ā. Afroozān Bāzghale and A. Mohammad-Khāh, "Improvement of Ultrasound-Assisted Removal of Rifampin in the Presence of N: ZnO/GO Nanocomposite as Sonocatalyst," *Chemistryselect*, Vol. 5 (15), pp. 4413-4421, 2020. https://doi.org/10.1002/slct.202000068.

[60] A. Khataee, P. Gholami, B. Kayan, D. Kalderis, L. Dinpazhoh, and S. Akay, "Synthesis of ZrO₂ nanoparticles on pumice and tuff for sonocatalytic degradation of rifampin," *Ultrasonics Sonochemistry*, Vol. 48, pp. 349-361, 2018. https://doi.org/10.1016/j.ultsonch.2018.05.008.

[61] D. Kanakaraju, B.D. Glass, and M. Oelgemöller, "Titanium dioxide photocatalysis for pharmaceutical wastewater treatment," *Environmental Chemistry Letters*, Vol. 12 (1), pp. 27-47, 2014. 10.1007/s10311-013-0428-0.

[62] S.O. Akpotu, E.O. Oseghe, O.S. Ayanda, A.A. Skelton, T.A.M. Msagati, and A.E. Ofomaja, "Photocatalysis and biodegradation of pharmaceuticals in wastewater: effect of abiotic and biotic factors," *Clean Technologies and Environmental Policy*, Vol. 21 (9), pp. 1701-1721, 2019. 10.1007/s10098-019-01747-4.

[63] H. Wang, X. Li, X. Zhao, C. Li, X. Song, P. Zhang, P. Huo, X. Li, "A review on heterogeneous

photocatalysis for environmental remediation: From semiconductors to modification strategies," *Chinese Journal of Catalysis*, Vol. 43 (2), pp. 178-214, 2022. https://doi.org/10.1016/S1872-2067(21)63910-4.

[64] H. Kais, N.Y. Mezenner, M. Trari, and F. Madjene, "Photocatalytic Degradation of Rifampicin: Influencing Parameters and Mechanism," *Russian Journal of Physical Chemistry A*, Vol. 93 (13), pp. 2834-2841, 2019. 10.1134/S0036024419130119.

[65] F. Soleimani and A. Nezamzadeh-Ejhieh, "Study of the photocatalytic activity of CdS–ZnS nano-composite in the photodegradation of rifampin in aqueous solution," *Journal of Materials Research and Techno*logy, Vol. 9 (6), pp. 16237-16251, 2020. https://doi.org/10.1016/j.jmrt.2020.11.091.

[66] R. Zou, T. Xu, X. Lei, Q. Wu, and S. Xue, "Novel and efficient red phosphorus/hollow hydroxyapatite microsphere photocatalyst for fast removal of antibiotic pollutants," *Journal of Physics and Chemistry of Solids*, Vol. 139, p. 109353, 2020. https://doi.org/10.1016/j.jpcs.2020.109353.

[67] N. Thuy Dang Thi, T. Ha Nguyen, V. Anh Ngo, T. Sen Nguyen, D. Dung Nguyen, and H. Nam Nguyen, " "Preparation and photocatalytic characterization of modified TiO$_2$/Nd/rice husk ash nanomaterial for Rifampicin removal in aqueous solution," *Environmental Science and Pollution Research*, 2022. 10.21203/rs.3.rs-581621/v1.

[68] G. Chen, "Electrochemical technologies in wastewater treatment," *Separation and Purification Technology*, Vol. 38 (1), pp. 11-41, 2004. https://doi.org/10.1016/j.seppur.2003.10.006.

[69] J. Wang and R. Zhuan, "Degradation of antibiotics by advanced oxidation processes: An overview," *Science of The Total Environment*, Vol. 701 (135023), 2020. https://doi.org/10.1016/j.scitotenv.2019.135023.

[70] I. Sirés and E. Brillas, "Remediation of water pollution caused by pharmaceutical residues based on electrochemical separation and degradation technologies: A review," *Environment International*, Vol. 40, pp. 212-229, 2012. https://doi.org/10.1016/j.envint.2011.07.012.

[71] L.R.D. Brito, S.O. Ganiyu, E.V. dos Santos, M.A. Oturan, and C.A. Martínez-Huitle, "Removal of antibiotic rifampicin from aqueous media by advanced electrochemical oxidation: Role of electrode materials, electrolytes and real water matrices," *Electrochimica Acta*, Vol. 396, p. 139254, 2021. https://doi.org/10.1016/j.electacta.2021.139254.

[72] M. Klavarioti, D. Mantzavinos, and D. Kassinos, "Removal of residual pharmaceuticals from aqueous systems by advanced oxidation processes," *Environment International*, Vol. 35 (2), pp. 402-417, 2009. https://doi.org/10.1016/j.envint.2008.07.009.

[73] D.P. Mohapatra, S.K. Brar, R.D. Tyagi, P. Picard, and R.Y. Surampalli, "Analysis and advanced oxidation treatment of a persistent pharmaceutical compound in wastewater and wastewater sludge-carbamazepine," *Science of The Total Environment*, Vol. 470-471, pp. 58-75, 2014. https://doi.org/10.1016/j.scitotenv.2013.09.034.

[74] M.E.T. Sillanpää, T. Agustiono Kurniawan, and W.-h. Lo, "Degradation of chelating agents in aqueous solution using advanced oxidation process (AOP)," *Chemosphere*, Vol. 83 (11), pp. 1443-1460, 2011. https://doi.org/10.1016/j.chemosphere.2011.01.007.

[75] D. Kanakaraju, B.D. Glass, and M. Oelgemöller, "Advanced oxidation process-mediated removal of pharmaceuticals from water: A review," *Journal of Environmental Management*, Vol. 219, pp. 189-207, 2018. https://doi.org/10.1016/j.jenvman.2018.04.103.

[76] S. Stets, B. do Amaral, J.T. Schneider, I.R. de Barros, M.V. de Liz, R.R. Ribeiro, N. Nagata, P. Peralta-Zamora, "Antituberculosis drugs degradation by UV-based advanced oxidation processes," *Journal of Photochemistry and Photobiology A: Chemistry*, Vol. 353, pp. 26-33, 2018. https://doi.org/10.1016/j.jphotochem.2017.11.006.

[77] A. Mukimin, H. Vistanty, and N. Zen, "Hybrid advanced oxidation process (HAOP) as highly efficient and powerful treatment for complete demineralization of antibiotics," *Separation and Purification Technology*, Vol. 241, p. 116728, 2020, https://doi.org/10.1016/j.seppur.2020.116728.

[78] Y. Orooji, A. Movahedi, Z. Liu, M. Asadnia, E. Ghasali, Y. Ganjkhanlou, A. Razmjou, H. Karimi-Maleh, N.T.H. Kiadeh, "Luminescent film: Biofouling investigation of tetraphenylethylene blended polyethersulfone ultrafiltration membrane," *Chemosphere*, Vol. 267, p. 128871, 2021. https://doi.org/10.1016/j.chemosphere.2020.128871.

[79] S. Arefi-Oskoui et al., "Development of MoS$_2$/O-MWCNTs/PES blended membrane for efficient removal of dyes, antibiotic, and protein," *Separation and Purification Technology*, Vol. 280, p. 119822, 2022. https://doi.org/10.1016/j.seppur.2021.119822.

[80] M.E. Casas, R.K. Chhetri, G. Ooi, K.M.S. Hansen, K. Litty, M. Christensson, C. Kragelund, H.R. Andersen, K. Bester, "Biodegradation of pharmaceuticals in hospital wastewater by staged Moving Bed Biofilm Reactors (MBBR)," *Water Research*, Vol. 83, pp. 293-302, 2015. https://doi.org/10.1016/j.watres.2015.06.042.

[81] S. Li, S. Zhang, C. Ye, W. Lin, M. Zhang, L. Chen, J. Li, X. Yu, "Biofilm processes in treating mariculture wastewater may be a reservoir of antibiotic resistance genes," *Marine Pollution Bulletin*, Vol. 118 (1), pp. 289-296, 2017. https://doi.org/10.1016/j.marpolbul.2017.03.003.